

# We are IntechOpen, the world's leading publisher of Open Access books Built by scientists, for scientists

6,900

Open access books available

186,000

International authors and editors

200M

Downloads

Our authors are among the

154

Countries delivered to

TOP 1%

most cited scientists

12.2%

Contributors from top 500 universities



WEB OF SCIENCE™

Selection of our books indexed in the Book Citation Index  
in Web of Science™ Core Collection (BKCI)

Interested in publishing with us?  
Contact [book.department@intechopen.com](mailto:book.department@intechopen.com)

Numbers displayed above are based on latest data collected.  
For more information visit [www.intechopen.com](http://www.intechopen.com)



# The Role of Quantum Dynamics in Covalent Bonding – A Comparison of the Thomas-Fermi and Hückel Models

Sture Nordholm<sup>1</sup> and George B. Bacskay<sup>2</sup>

<sup>1</sup>*The University of Gothenburg*

<sup>2</sup>*School of Chemistry, The University of Sydney*

<sup>1</sup>*Sweden*

<sup>2</sup>*Australia*

## 1. Introduction

### A brief history of thoughts on covalent bonding

The mechanism of covalent bonding is the basis of molecule formation and therefore of all of chemistry. It is a phenomenon which is extremely well characterized experimentally. The properties of covalently bonded molecules can also be reproduced and/or predicted by increasingly accurate calculations using the methods of quantum chemistry. These days, such calculations can be routinely performed using commercial program packages which are readily available to all chemists, who frequently find that molecular properties are simpler to calculate than to measure or track down in the literature. In the light of this success it is remarkable that the physical explanation of the origin of covalent bonding is still a subtle and contentious issue generating much discussion. The aim of this chapter is to reveal the origin of covalent bonding in simple terms and with illustrations allowing subtleties to be clarified and arguments to be settled. We shall propose that a deeper and more general analysis than hitherto widely known shows the merit and limitation of previous explanatory models and offers important clues for the understanding of the present computational methods of quantum chemistry and their future development. Our discussion will employ two very simple but very different theories of electronic structure – the Thomas-Fermi theory and the Hückel model of planar conjugated hydrocarbon molecules – which contain within them a full range of the dominant mechanisms needed to describe covalent bonding. The analysis presented here is in turn based on earlier articles [1-6] and a thesis which is not yet published in all its essential parts [7].

A brief historical review of the understanding of covalent bonding is in order. The first model of covalent bonding which remains very relevant today is that of Lewis who understood that the periodic variation in chemical stability of the elements was the origin of chemical bonding and of the covalent bonding mechanism in particular [8]. The model of Lewis suggested that atoms which do not have an inert gas like electronic structure seek to achieve such a structure and its particular stability by either electron transfer between atoms, forming ionic bonds, or by electron sharing in forming covalent bonds between

atoms in molecules. The Lewis diagrams can be used to identify the bonds formed. Both mechanisms are in principle always present but more or less applicable and nature seems to confirm that molecules with very obvious Lewis structures according to ionic (valence electron transfer) or covalent (valence electron sharing) mechanisms are particularly stable. In our view the Lewis model – at its simple level without reference to any form of mechanics – is valid and useful. The difficulties start when one tries to interpret the bonding mechanisms identified by Lewis in more mechanical terms.

The ionic bonding mechanism lends itself readily to a mechanical interpretation. One needs only to note that ionic bonds form when the electron transfer to create inert gas like ions at infinite separation requires relatively little energy since electron affinities and ionization energies are unusually close. Once the ions have formed one can then estimate the binding energy released when they approach to form an ionic structure. Doing this for, e.g., NaCl, gives a good prediction of the ionic bond strength. One immediately also understands that such ionic molecules are very reactive due to their polar nature and form extended crystal structures rather than inert molecules. Thus the ionic bonding mechanism is very simple to understand in terms of well known properties of the atoms. The complicating quantum mechanical effects are hidden in the properties of the atoms and reflected in the periodically variable ionization energies and electron affinities.

The covalent bonding mechanism presents a far more difficult case. The physical explanation is still debated despite the apparent truth of the Lewis electron sharing model and the ability of modern quantum chemistry to account for the bond strengths to great accuracy. The question is how to physically interpret the calculations based on the quantum mechanical Schrödinger equation for the electronic structure of atoms and molecules. A first significant interpretation was offered by Hellman [9] already in the 1930-s soon after quantum mechanics had been developed. He suggested that covalent bonding should be understood as a quantum mechanical effect due to the lowering of ground state kinetic energy associated with the delocalization of valence electron motion between atoms in the covalently bound molecule. Although we shall find much which is correct in this proposal the picture is clouded by apparently contradictory facts. Most chemists at the time were reluctant to assign covalent bonding to a quantum effect. Instead the idea, seemingly supported by the Lewis diagrams with their electron pairs placed between bonded atoms, that electrostatic interaction between these pairs and the positively charged atomic centers in the molecule was the origin of the covalent bond became favored by most authors of introductory texts on chemistry. This view was supported by Coulson who in his famous book *Valence* [10] in 1961 pointed to the Virial Theorem of Coulombic systems which showed rigorously that when a molecule in its equilibrium (lowest energy) configuration was formed from infinitely separated atoms the kinetic energy rises by half as much as the potential energy drops. Thus it appeared that kinetic energy – in complete disagreement with Hellman's proposal – opposed bonding while the electrostatic interactions were the cause of bonding. It seemed therefore that the covalent bonding mechanism could be understood as an extension of the ionic bonding mechanism to include the effect of electron pairs located at bond midpoints between atoms. In more detailed discussions bond formation was seen to be associated with excess electron density placed around bond midpoints by constructive overlap of atomic orbitals in bonding molecular orbitals. For more recent elaboration of the electrostatic view of the mechanism of covalent bonding see, e.g. a book by Burdett [11] and an essay by Bader and coworkers [12].

This view of covalent bonding as an electrostatic interaction was generally accepted among chemists even though Ruedenberg [13] already in 1962 showed that the Virial Theorem was in small molecules like  $\text{H}_2^+$  and  $\text{H}_2$  a reflection of orbital contraction, i.e., the tightening of the electron density around the two nuclei rather than the displacement of electron density into the region around the bond midpoint. Ruedenberg suggested that this contraction of atomic orbital or electron density around the atomic nucleus could be thought of as a “promotion” of the atom to a smaller size appropriate in the molecule. If this promotion was performed at a certain cost in increased energy at infinite separation then the subsequent formation of the molecule would follow the proposal of Hellman and show a decrease in kinetic energy due to valence electron delocalization which stabilizes the bond. An alternative procedure followed by most early applications of quantum chemistry to the calculation of covalent bond energies is to use frozen atomic orbitals in a minimal basis set calculation in which case the orbital contraction identified by Ruedenberg is completely absent. In this case the Virial Theorem is completely violated in the bond formation which is again – as predicted by Hellman – due to the lowering of the kinetic energy upon electron delocalization. One may then – as suggested by Kutzelnigg [14]– at the end of such a calculation allow the orbital exponents reflecting degree of contraction around the nuclei to be optimized. The Virial Theorem now is satisfied but only a small decrease in both total energy and bond length is found. Thus one can see that the ability to resolve the covalent bonding mechanism is hardly dependent on whether the Virial Theorem is satisfied or only weakly so. Recent discussion of this issue can be found in articles by Ruedenberg [15] and Kutzelnigg [16] and work cited therein.

## 2. The current impasse

The problem we are currently faced with in the understanding of covalent bonding is that we have a well formed empirical concept of a covalent bond which is arguably the very foundation of chemistry and we have within modern quantum chemistry many approximate theories which allow us to compute the structures, energies and other properties of covalently bonded molecules with high and ever increasing accuracy. Remarkably we still have not agreed upon how to provide an appropriate physical explanation of the observed and calculated covalent bonding. Clearly the arguments of Hellman and Ruedenberg in terms of kinetic energy lowering and that of Coulson and many authors of chemistry textbooks in terms of electrostatic interactions as the source of covalent bonding have their “grains of truth” but they also contain apparent contradictions which may confuse students or make textbook authors avoid the issue of physical understanding of covalent bonding altogether.

Most quantum chemists appear to be pragmatic about this state of affairs and are not greatly concerned with the lack of physical understanding as long as their methods can quantitatively resolve covalent bonding. Bader [12] and others strongly maintain that chemical bonding must be thought of as due to an electrostatic interaction connected with the redistribution of electron density to yield a build up in the interatomic ( $\sim$  bond midpoint) region. Others, e.g. Frenking, [17] seek insight into chemical bonding from an energy decomposition analysis (EDA) using the results of modern quantum chemistry for molecules with various types of chemical bonds. This can be thought of as a refinement of the discussion about the roles of kinetic or potential energies and whether one or the other is

the key to the covalent stabilization. There are of course different types of kinetic and potential energies. While contributing insight, these interpretations of modern quantum chemistry have not provided a convincing and fully accepted resolution of the dispute concerning the nature of covalent bonding. Our own work over a period of 25 years [1-6] has pointed to a deeper quantum dynamical origin of covalent bonding. This work has departed significantly from earlier mechanistic interpretations of covalent bonding, but thus far it has had little impact on the earlier and long-held views of the mainstream chemical community. It is this both general and more personal impasse which forms the starting point of our present contribution.

### **3. The present focus – The nonbonding of Thomas-Fermi Theory contrasted with the successful bonding model of Hückel Theory**

Our view proposed here in the light of a long program of research is that i) there is a need for a deeper physical understanding of covalent bonding, ii) such an understanding will show that covalent bonding is a dynamical phenomenon relating to the motion of valence electrons in the molecule and iii) this insight casts helpful new light on the range of chemical bonds in molecules and materials and the applicability of quantum chemical methods in the calculation of atomic reactivity and covalent bonding. The aim here is to expose the main points of our analysis in their simplest context. Thus we focus on two old and simple methods, i.e., the original electronic density functional theory of Thomas and Fermi [18, 19] and the Hückel model of  $\pi$ -electron states in planar conjugated hydrocarbon molecules [20]. TF theory is known [21, 22] to fail completely to describe covalent bonding while the Hückel model is the simplest approach to the calculation of covalent bonds and provides within it a pedagogical illustration of the generality of its underlying mechanism [23].

The complete failure of Thomas-Fermi (TF) density functional theory (DFT) with respect to covalent bonding is also a very significant advantage in the search for the mechanism of covalent bonding. The TF DFT is in many ways very successful and it contains representation of all the major electrostatic forces proposed as the origin of covalent bonding. Its variable electron density can clearly be made to reflect excess density at bond midpoints and in bonding regions between nuclei in molecules. Yet it returns no covalent bonding whatsoever. It would appear there must be a fundamental reason for this which in turn may tell us what covalent bonding is really about.

The Hückel theory of  $\pi$ -electron resonance stabilization is – in stark contrast – almost inexplicably successful at capturing covalent bonding. It is fundamentally a quantum mechanical theory of one-electron wave functions, the  $\pi$ -molecular orbitals. The empirical form of its one-electron Hamiltonian is exceedingly simple. The bonding is essentially captured by one parameter  $\beta$ , which is placed off-diagonally, so as to allow the formation of band-like molecular orbitals delocalized over the planar hydrocarbon structure. There would not appear to be any room for the intricacies of virial theorems or electron density rearrangement to bond midpoints or bonding regions. Yet the  $\pi$ -bonding of two carbon atoms in ethylene or the resonance in benzene seem well resolved by this simple theory.

It will be our premise here that the mechanism of covalent bonding can be identified by noting first that it is contained in the error made by the Thomas-Fermi theory in representing quantum mechanics and secondly noting that whatever this error is it is not



affecting the Hückel model of  $\pi$ -bonding. Covalent bonding, whether normal or resonant in character, is clearly contained in this model with extensions to  $\sigma$ -electrons and its nature should therefore be deducible from the simple ansatz of the Hückel theory. In mathematical terms the mechanism has been captured in the intersection of (1) the complement to the TF theory and (2) Hückel theory.

#### 4. Thomas-Fermi Theory – Quantization by the semiclassical Correspondence Principle

Thomas-Fermi (TF) theory is the original density functional theory (DFT) of electronic structure. It proposes that the ground state energy of electrons in an external potential  $V_{\text{ext}}(\mathbf{r})$  can be found by minimizing the functional –

$$E(\rho) = C \int d\mathbf{r} [\rho(\mathbf{r})]^{5/3} + \frac{1}{2} \int d\mathbf{r} \rho(\mathbf{r}) \int d\mathbf{r}' \rho(\mathbf{r}') / r_{12} + \int d\mathbf{r} \rho(\mathbf{r}) V_{\text{ext}}(\mathbf{r}) \quad (1)$$

where atomic units have been used such that  $C$  is  $3(3\pi^2)^{2/3}/10$  and the Coulomb interaction between two electrons appears as  $1/r_{12}$  with  $r_{12}$  being the separation between the electrons. The first term on the right is the kinetic energy functional, the second is the electrostatic repulsion between electrons and the third is the potential energy of interaction with the external field  $V_{\text{ext}}(\mathbf{r})$ . It should immediately be noted that this – in distinction to most modern forms of DFT – is a true density functional in that no reference is made to any wave function. Thus solving for ground state electronic structure and energy is far simpler in TF theory than in modern DFT where Kohn-Sham or Hartree-Fock expressions are used for the kinetic energy with the introduction of one-electron orbital wave functions. Many features of electronic structures are well reproduced by solutions obtained by TF theory but the failures are also dramatic. Given that covalent bonding is completely absent TF theory eliminates chemical reactivity and thereby nearly all of chemistry. Beyond that singular failure lie quantitative errors – particularly for small systems.

A full derivation of TF theory can be carried out by semi-classical arguments mapping quantum mechanics into classical phase space by the following assumptions:

1. Each quantum state of an electron corresponds precisely to a phase space volume of  $h^3$ .
2. Each one-electron energy eigenstate can be found by sequentially slicing up classical phase space by energy surfaces separated by a phase space volume  $h^3$ . The phase space slices so formed are uniformly occupied and the energy of the corresponding quantum energy eigenstate is the uniform slice average of the classical energy.
3. The formation of classical quantum states is carried out ergodically, i.e., without considering any possible dynamical constraints that may decompose phase space. The electronic phase space is extended to have a spin up and a spin down half-space which are both included in the summation to find the state volume  $h^3$ .
4. Many-electron systems are assumed to satisfy the mean-field approximation where the individual electrons are moving independently in an average field created by all electrons.

The details can be found in a thesis [7] and will be published independently. Here we want to point out how the known errors and limitations of TF theory enters through the construction of the functional on this semiclassical basis. A good summary of the

performance of Thomas-Fermi theory for atoms and molecules can be found in the book by Parr and Yang on “The Density-Functional Theory of Atoms and Molecules” [24] where also many correction schemes have been discussed. It is our purpose here to reveal as clearly as possible the underlying causes of the failure of the original TF theory – particularly the reason why atomic reactivity and covalent bonding are absent. It then becomes possible to not only understand how to correct the theory but also to identify the origin of atomic reactivity and the covalent bonding mechanism in its general form.

#### 4.1 Thomas-Fermi Theory for one-dimensional motion

We begin by considering the familiar particle-in-the-box system where a single electron is moving in a potential  $V(x) = 0$  for  $0 < x < L$ , and  $= \infty$  elsewhere. Given the classical kinetic energy  $T = p^2/2m$  it is clear that the classical phase space volume below an energy  $E$  is  $\Omega(E) = 2p(E)L = 2(2mE)^{1/2}L$  and the density of states is  $\rho(E) = (2m/E)^{1/2}L$ . The energies separating states are obtained from  $\Omega(E_{F,n}) = nh$ , which yields  $E_{F,n} = (nh/2L)^2/2m$ . Finally the TF energy eigenvalues are obtained as –

$$E_n^{(\text{TF})} = h^{-1} \int_{E_{F,n-1}}^{E_{F,n}} dE \rho(E) = \frac{h^2 \left( n^2 - n + \frac{1}{3} \right)}{8mL^2} \quad (2)$$

This result strongly resembles the exact relation  $E_n = h^2 n^2 / 8mL^2$  as shown in Figure 1, but the TF result is always slightly lower.

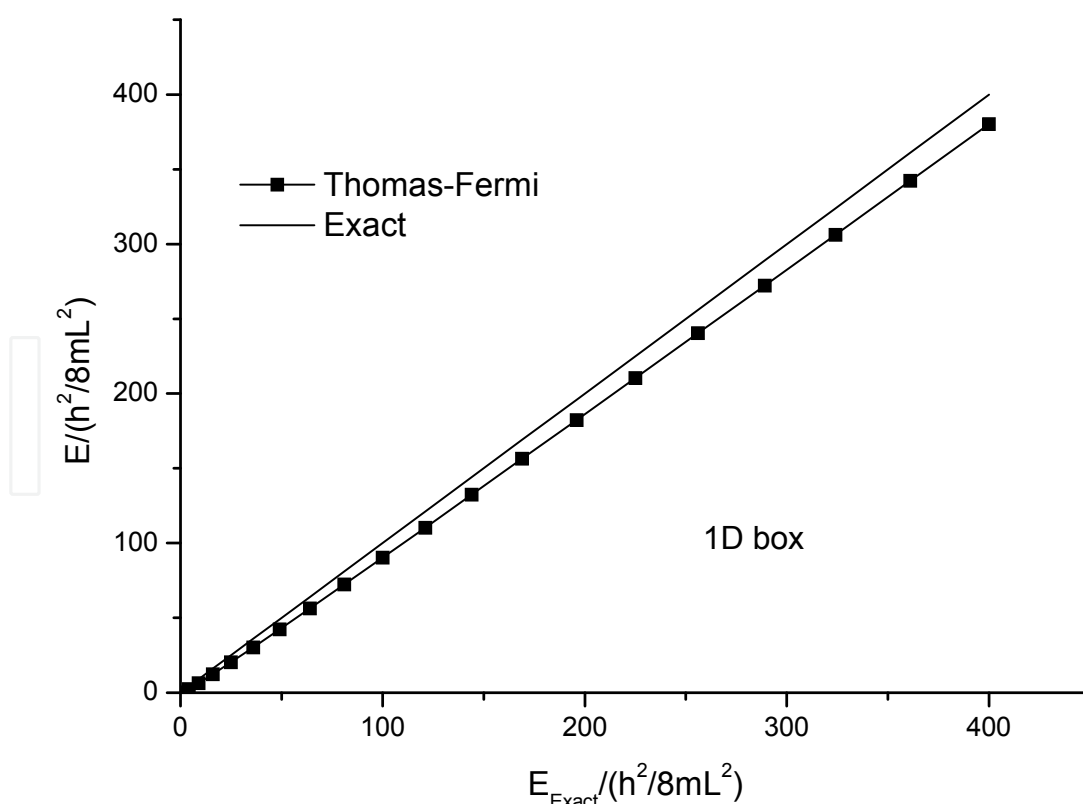


Fig. 1. Comparison of Thomas-Fermi (filled square) with exact (diagonal line) 1D particle-in-the-box energy eigenvalues

In fact we note that  $E_{F,n} = E_n$  so that the exact result is the upper bound on the slice of phase space making up the TF energy eigenstate. The reason for this deviation is that the correct quantum energy has a component of gradient kinetic energy which sets in as the wave function is brought to zero at the hard walls defined by the rise of the potential to infinity. The TF energy lacks this type of gradient kinetic energy and allows the density to be constant  $1/L$  in the interval  $[0, L]$  rather than of the form  $2\sin^2(\pi x)/L$  which vanishes at both endpoints with a peak in the middle.

The gradient kinetic energy is related to the change in motion and thereby to the dynamical mechanism that TF theory completely neglects. It is easily shown that only this type of gradient kinetic energy arises for electrons in ground state orbitals and it can be obtained in terms of the electron density by a functional first noted by von Weizsäcker [25]. For many-electron systems where more than the ground state orbital is filled there is another type of kinetic energy which we might call “orthogonality kinetic energy”. It is directly connected with the Pauli principle and the Pauli repulsion between molecules. In the semi-classical derivation of TF theory one can see that the TF kinetic energy functional is estimating orthogonality kinetic energy but in a way that extends it also to one or two electron ground states. Interestingly the TF estimate of the energy levels of a harmonic oscillator in one dimension is in perfect agreement with the exact result (see Figure 2). This is due to a cancellation of the gradient kinetic energy rise and the lowering of energy that follows from the tunneling of orbital wave functions into the potential wall.

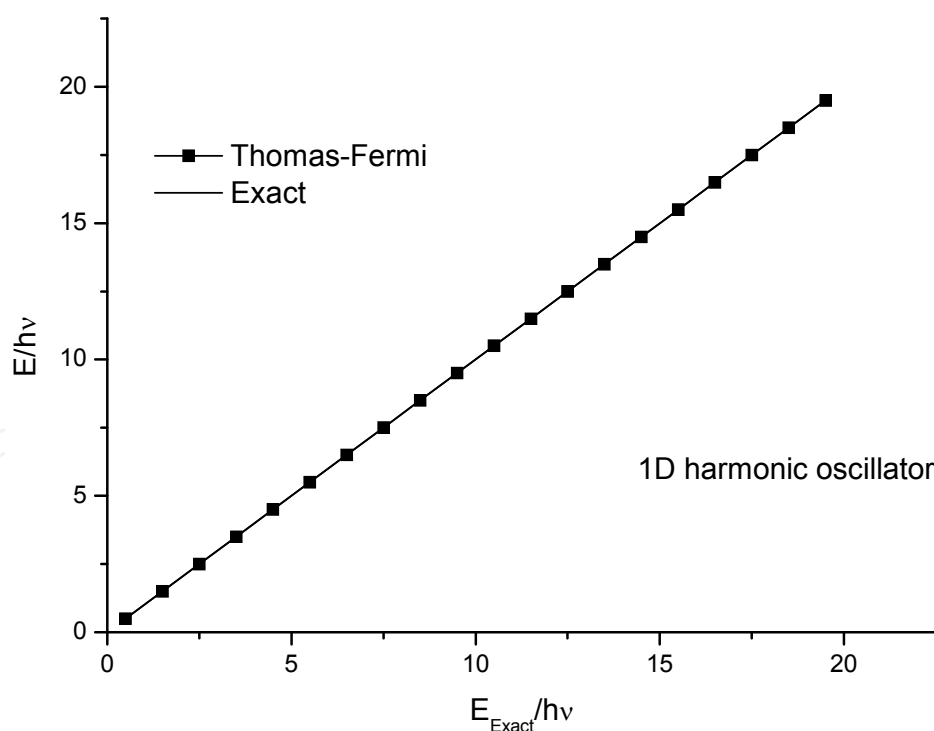


Fig. 2. Comparison of Thomas-Fermi (filled squares) with exact (diagonal line) energy eigenvalues for the 1D harmonic oscillator.

If we consider electron motion in a three dimensional cubic box we find two types of errors in the TF results compared with exact results as shown in Figure 3. The TF energies are



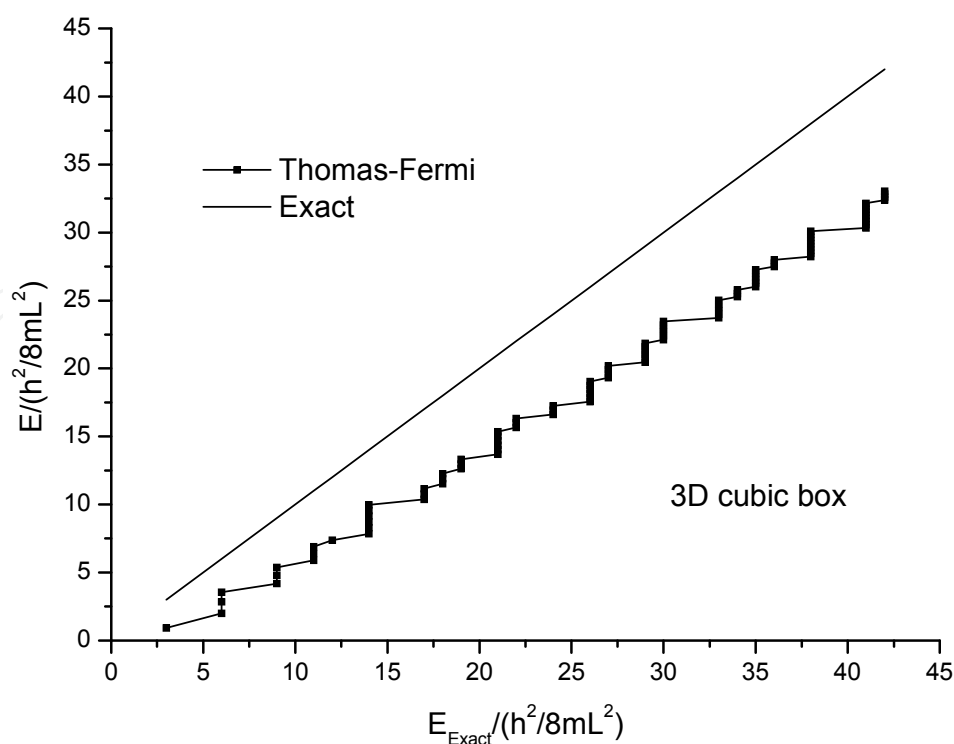


Fig. 3. Comparison of Thomas-Fermi (filled squares forming jagged line) and exact (diagonal line) energy eigenvalues for the cubic box potential in 3D.

generally too low due to the lack of gradient kinetic energy but they are also nondegenerate and smoothly progressing with decreasing energy gaps while the exact results show larger and very variable energy gaps but strong degeneracies of the energy levels.

The same comparison of exact and TF energies for the isotropic 3D harmonic oscillator in Figure 4 show only this latter error where the TF energy levels are nondegenerate with smoothly decreasing energy gaps while the exact spectrum shows constant energy gaps as for the 1D harmonic oscillator but rapidly rising degeneracy.

The “degeneracy deficiency” seen in the TF eigenvalues of both the particle-in-the-cube and the isotropic 3D harmonic oscillator is due to the assumption of rapid ergodic electron dynamics which ignores the separability of the  $x$ ,  $y$  and  $z$ -directed motion of the electron in these two potential wells. If we were to account for this separability and apply the TF theory to each 1D motion in the axial directions independently then the degeneracies would be recovered and we would have perfect agreement between 3x1D TF results and exact results for the harmonic oscillation and only the gradient error remaining in the case of the motion in a cube as shown in Figure 3.

The identification of the “dynamical error” in standard TF theory above is of the utmost importance since the degeneracies in the spectra of the electron motion in a cube or in an isotropic 3D harmonic oscillation are a reflection of what we call “shell structure” in the case of atoms. Thus we can see already that the TF theory ignores shell structure and we shall show below that it thereby also ignores atomic reactivity. In order to correct TF theory for this error we need to explicitly account for the dynamical constraints, i.e. non-ergodicity and hindered electron dynamics, which is present in real electronic structures. This is easy to do

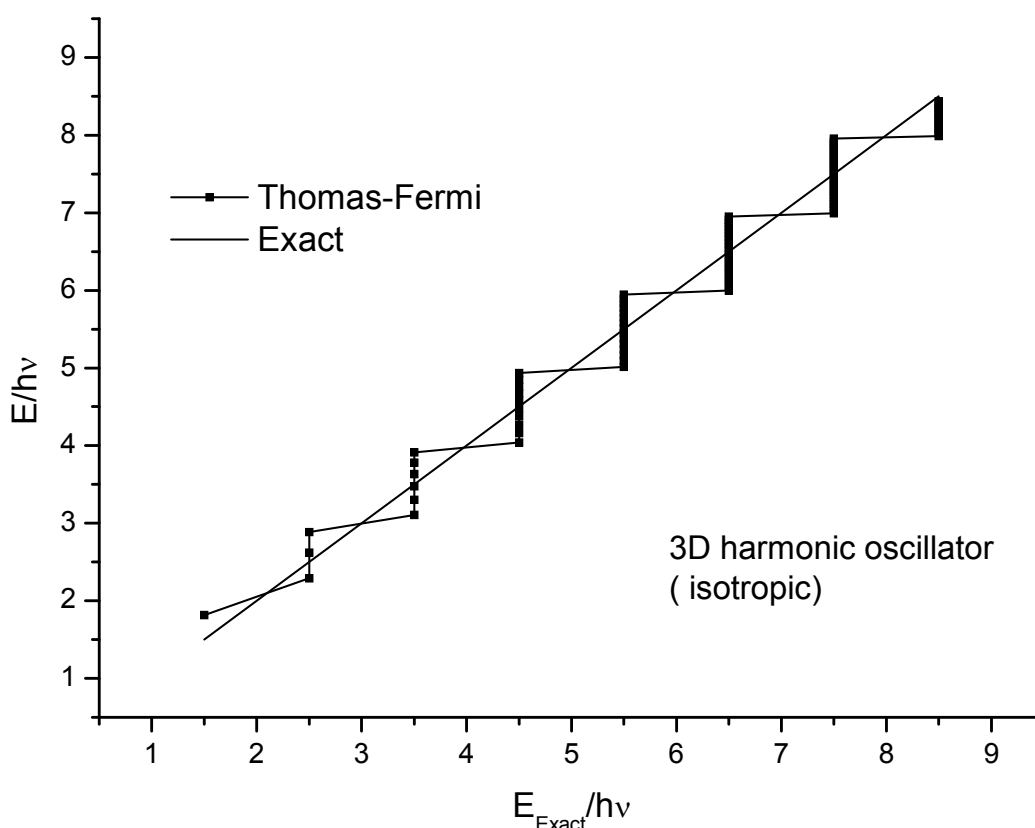


Fig. 4. Comparison of Thomas-Fermi (filled squares in jagged line) and exact (diagonal line) energy eigenvalues for the isotropic 3D harmonic oscillator.

in the case of separable electronic motion as above but will be more subtle below as we approach realistic atomic and molecular systems.

The dynamical error illustrated above can be seen to be related to the loss of shell structure in the TF theory. The molecular dynamical error which eliminates covalent bonding can be illustrated for motion in a simple one-dimensional double well potential:

$$\begin{aligned}
 V(x) &= \infty, \quad x < -(L+a)/2 \quad \text{or} \quad x > (L+a)/2 \\
 &= 0, \quad -(L+a)/2 \leq x \leq -a/2 \quad \text{or} \quad a/2 \leq x \leq (L+a)/2 \\
 &= V_0, \quad -a/2 < x < a/2
 \end{aligned} \tag{3}$$

This potential is shown in Figure 5.

With a barrier height of  $2.0 E_h$  (5.25 MJ/mol) and  $L = 8.0 a_0$  (4.23 Å) the energy splitting between the ground and first excited state energies according to TF theory, is compared with the exact result  $\Delta E_{21} (= 3h^2/8mL^2$  for  $a = 0$ ) in Figure 6.

We see that while the exact result – as is well known – is very sensitive to the barrier width  $a$ , the TF result is always the same irrespective of barrier width. Thus near degeneracies in molecular spectra of orbital energies are not accounted for in TF theory. Such near degeneracies are related to hindered electron motion between the two wells and thus to the reactivity of the system. In the case of interacting atoms this type of near orbital degeneracy is relaxed as the atoms bond by the covalent mechanism. Thus the formation of the covalent

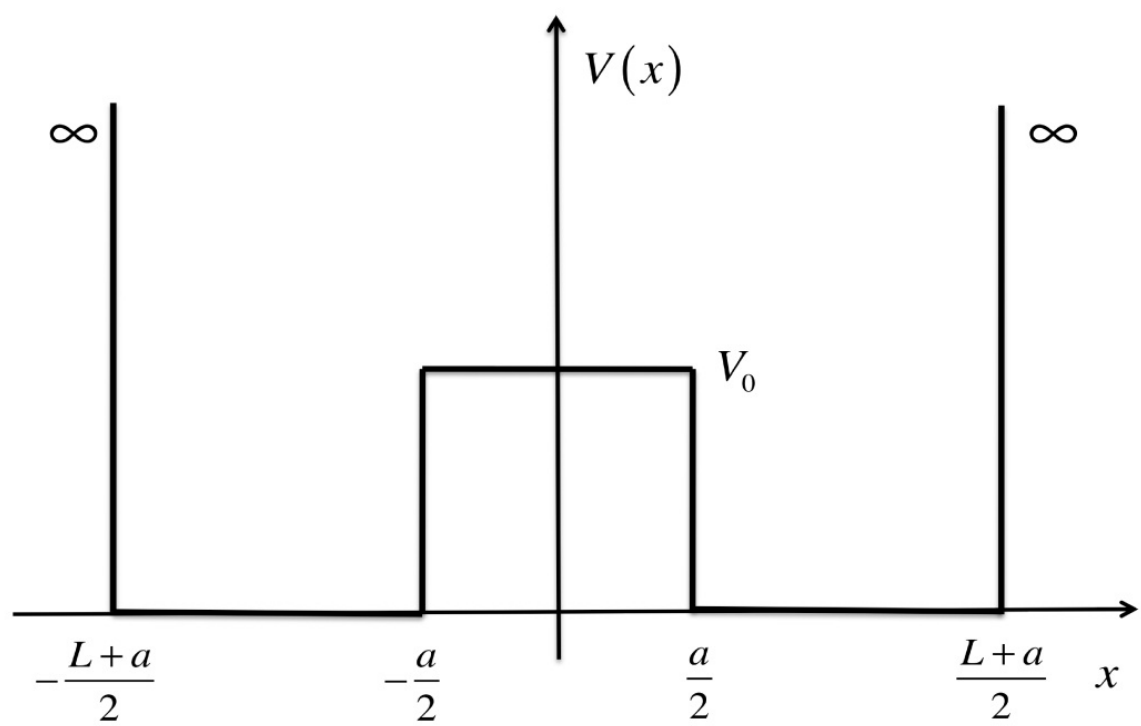


Fig. 5. The 1D double square well potential.

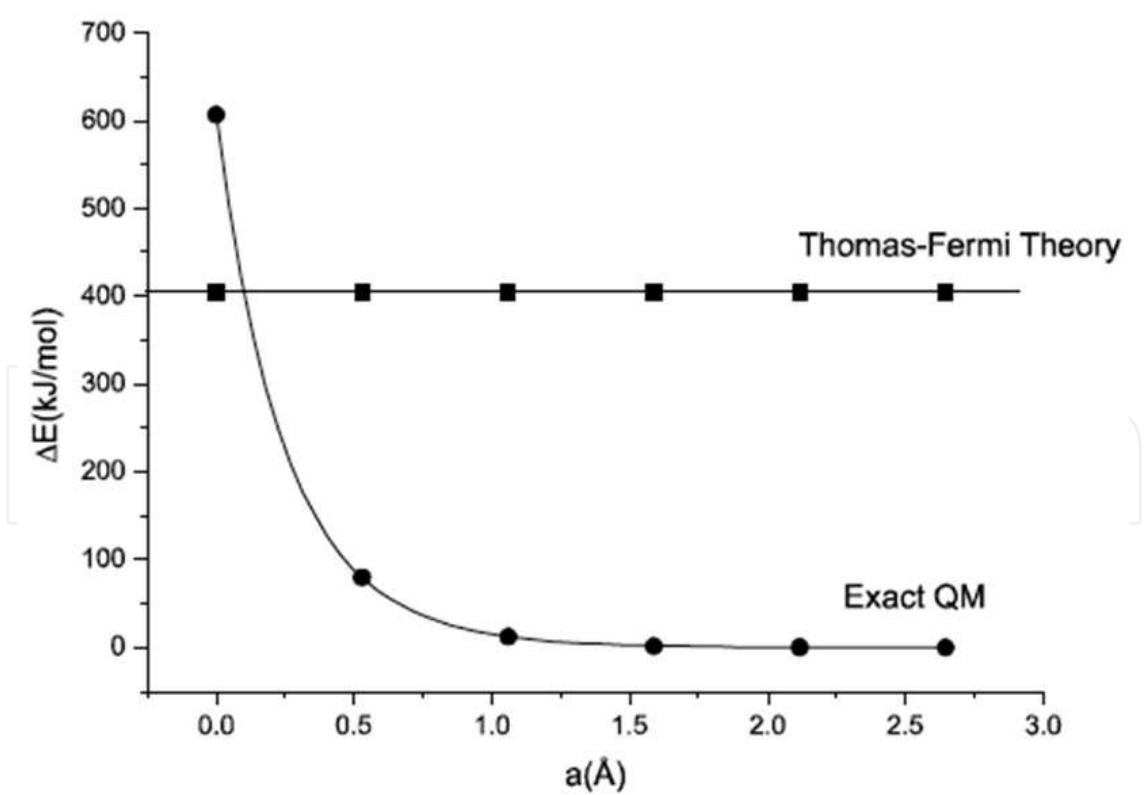


Fig. 6. Comparison of the energy splitting between ground and first excited states of a double square well motion in one dimension. The TF theory shows constant and large splitting while the exact result decreases rapidly towards zero with increasing barrier width.

bond will be found to be directly related to the facilitation of interatomic electron transfer which is reflected in the transition of the energy spectrum of the separated atoms from degenerate or near degenerate form towards a nondegenerate form for molecules as in the TF theory. The failure of TF theory to describe covalent bonding is then clearly due to the ergodic quantization procedure which produces smooth progression of electronic energy levels without degeneracies or near degeneracies at all atomic separations.

4.2 The hydrogen atom

In the case of the hydrogen atom (in atomic units) the 3D potential is –

$$V(r) = -1/r .$$

(4)

The phase space volume below the energy E can be worked out analytically as

$$\Omega(E) = 2^{3/2}\pi^3/3(-E)^{3/2} .$$

(5)

The energy eigenvalues according to Thomas-Fermi theory readily follow and are shown compared with the exact energy eigenvalues of the hydrogen atom in Figure 7. We have

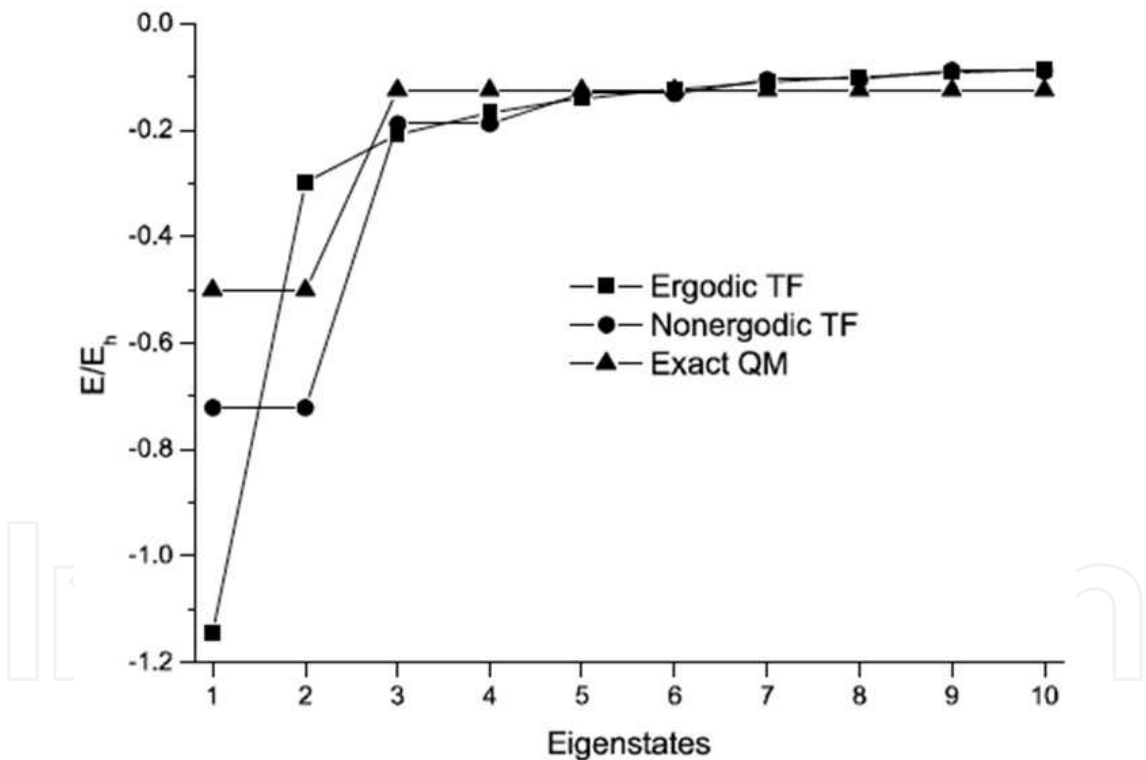


Fig. 7. Comparison of Thomas-Fermi and exact energy eigenvalues for the hydrogen atom. The original TF theory is called “ergodic” while the spin-conserving TF theory is denoted “nonergodic”.

$$E_n^{(TF)} = -2^{1/2}(2^{1/2}/12)^{-1/3}/4 \text{ for } n = 1,$$

(6)

$$= [-2^{1/2}(2^{1/2}/12)^{-1/3}/4] \times [n^{1/3} - (n - 1)^{1/3}] \text{ for } n = 2,3,\dots$$

(7)

as compared to the exact values –

$$E_{n,l,m} = -1/2n^2, n = 1, 2, \dots, l = 0, 1, \dots, n-1, m = -l, -l+1, \dots, l-1, l. \quad (8)$$

However, the electron has spin – either up or down. We have so far considered spinless particles. Allowing for spin while maintaining the ergodic quantization of the original TF theory will double the phase space as the electron is allowed to rapidly flip from up to down or vice versa. The results above therefore describe doubly degenerate energy levels which correspond to a form of “nonergodic” TF theory which conserves spin. The standard TF theory, on the other hand, will populate both spin up and spin down phase space with one-electron states which are spin-depolarized giving nondegenerate energy levels. Figure 7 shows both the fully ergodic (original) TF energy eigenvalues as well as those obtained by the spin-nonergodic TF theory described above. The clear picture seen is that the Thomas-Fermi energies behave reasonably apart from the inability to resolve the highly degenerate shell structure of the correct quantum results. This will be a key fact in the resolution of reactivity and covalent bonding proposed below.

### 4.3 The hydrogen molecule ion

The simplest molecule, the hydrogen molecule ion  $H_2^+$ , has an electronic potential composed of two displaced hydrogen atom potentials, hence the total potential energy including the internuclear repulsion (all in atomic units) is -

$$V(r) = -\frac{1}{r_a} - \frac{1}{r_b} + \frac{1}{R} \quad (9)$$

where  $r_a$  and  $r_b$  represent the distance of the electron from nuclei  $a$  and  $b$  respectively and  $R$  is the internuclear separation.

The first two terms in equation (9) correspond to a double well potential of two superposed hydrogen Coulomb wells while the third term represents the repulsion between the two protons. The integral determining the phase space volume below an energy  $E$ ,  $\Omega(E)$ , is now harder to find analytically but still easy to determine numerically. We leave those details aside and consider the results obtained by the “nonergodic” (i.e., spin conserving) form of Thomas-Fermi theory. In Figure 8 we show the electronic, internuclear and total energy of the ground state as a function of the internuclear separation  $R$ .

It is clear from the figure that while the electronic energy is weakly attractive the internuclear repulsion is stronger and the total energy is weakly repulsive. The phase space integrations are readily extended to generate excited state energies and the corresponding bond energy curves for the first ten states of  $H_2^+$  in the spin conserving TF theory are shown in Figure 9 below.

The non-bonding character of the Thomas-Fermi results is not related to the choice of spin conserving or original spin-unpolarized theory. As will be even more clear after consideration of the successfully bonding Hückel theory below the problem of the Thomas-Fermi theory is related to the inability to resolve the constraints on the electron dynamics. In the case of the calculations for  $H_2^+$  above the loss of bonding is related to the inability to resolve left-right electron transfer between the two coulombic potential wells located on the protons. As seen very clearly in the case of the two non-overlapping square wells in 1D above the TF theory will effectively quantize the motion as if the dynamical hindrance of the

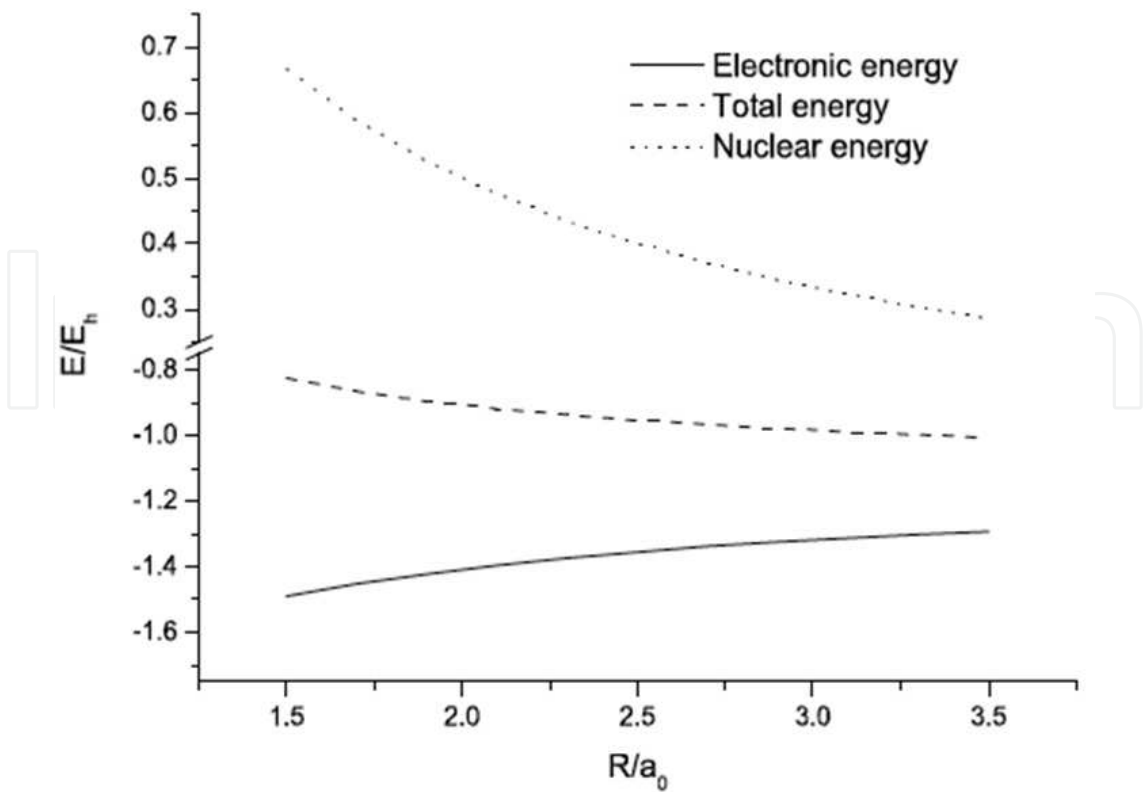


Fig. 8. The Thomas-Fermi energies for  $H_2^+$  obtained in the “nonergodic” (spin conserving) theory are shown as a function of bond length  $R$ . From the top we have the internuclear, total and electronic energies.

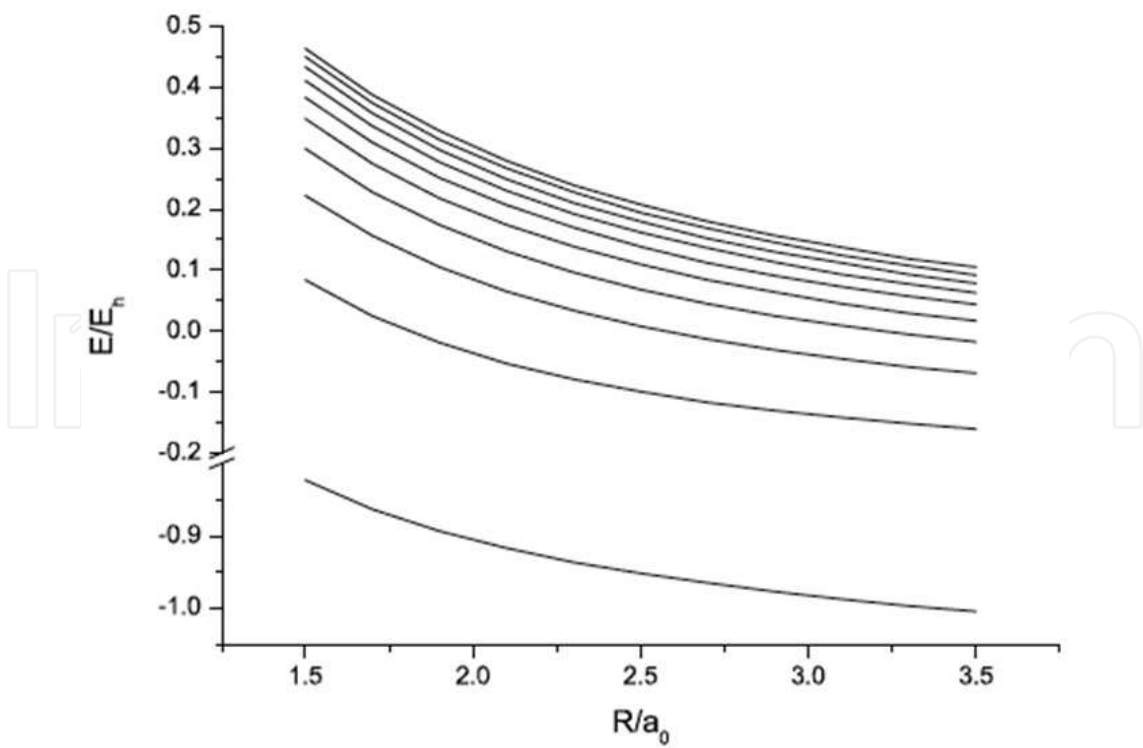


Fig. 9. Total energies for the lowest ten states of  $H_2^+$  in the spin conserving form of Thomas-Fermi theory.



barrier was not present – irrespective of its width. In the same way the TF results for  $H_2^+$  above have a character as if the electron transfer is rapidly delocalized for all bond lengths in stark contrast to the slowing down of this transfer by an increasingly broad barrier for increasing bond length seen in the exact quantum mechanical results. This will be discussed in greater detail in connection with the Hückel model below.

We conclude this examination of the Thomas-Fermi theory with the observation that it is able to follow broad trends in the density of energy eigenstates quite well but fails to resolve degeneracies and near-degeneracies in the spectrum due to dynamical conservation laws and other constraints such as potential barriers penetrable only by tunneling. In order to confirm our notion that this failure is also the cause of its inability to predict covalent bonding we now turn to the Hückel theory which despite its simple empirical nature is able to resolve covalent bonding very well. We shall particularly consider the representation of dynamics afforded by the Hückel theory to find therein the reason why it succeeds where the Thomas-Fermi theory fails.

## 5. Covalent bonding as described by the Hückel Molecular Orbital (HMO) model

Hartree-Fock and modern DFT based on the Kohn-Sham kinetic energy both successfully describe covalent bonding – albeit with some quantitative errors due to incorrect description of electron correlation effects. Common to these theories is the key role played by molecular orbitals formed from modified atomic orbitals as the covalently bound molecule is created. It is clearly the nature of these molecular orbitals and their orbital energies which carries the information about the covalent bonding mechanism. In order to most graphically illustrate the covalent bonding mechanism we shall therefore reexamine perhaps the simplest form of molecular orbital quantum chemistry, the Hückel molecular orbital model, which successfully captures the covalent bonding mechanism. In particular we shall

- claim that Hückel theory, appropriately interpreted and extended, is the minimal and precisely focussed explanation of all forms of covalent bonding,
- use the Hückel model to illustrate the concept of quantum ergodicity in the context of electron dynamics,
- show that Hückel theory displays the direct relation between electron delocalization and quantum ergodicity which in turn is the key to covalent bonding, and
- argue that all main types of bonding, including resonance stabilization, can be systematically organized according to the degree of delocalization employed in the stabilization.

The molecular orbitals (MO) of a molecule are, by definition, solutions of the Hartree-Fock equations, i.e. eigenfunctions of the Fock operator

$$\hat{F}\psi_i = \varepsilon_i\psi_i \quad (10)$$

where  $\hat{F}$  is an effective one-electron Hamiltonian operator for a single electron within the molecule which interacts with the nuclei and all other electrons. Thus we have

$$\hat{F} = \hat{T} + \hat{V}_N + \hat{J} - \hat{K}, \quad (11)$$

where  $\hat{T}$  is the kinetic energy operator of an electron,  $\hat{V}_N$  and  $\hat{J}$  represent the Coulomb interaction of an electron with the nuclei and all other electrons respectively, and  $\hat{K}$  is the exchange operator which accounts for the fermion nature of the electrons, i.e. the anti-symmetry requirement on the total many-electron wave function. In the majority of quantum chemical applications the MO-s are constructed from atom centred basis functions  $\{\chi_k\}$ ,

$$\psi_i = \sum_k C_{ki} \chi_k. \quad (12)$$

The Hartree-Fock equations, when projected onto the space spanned by the above atomic orbital (AO) basis, become matrix eigenvalue equations

$$\mathbf{FC} = \mathbf{SC}\epsilon, \quad (13)$$

where  $\mathbf{S}$  and  $\mathbf{F}$  are the overlap and Fock matrices,

$$S_{kl} = \langle \chi_k | \chi_l \rangle, \quad (14)$$

$$F_{kl} = \langle \chi_k | \hat{F} | \chi_l \rangle. \quad (15)$$

The Hückel MO method is developed from Hartree-Fock theory through a series of assumptions and approximations.

1. As Hückel theory was formulated primarily for conjugated hydrocarbons, i.e. planar molecules, the  $\sigma - \pi$  separability applies and hence the Fock equations are block-diagonal:

$$\begin{pmatrix} \mathbf{F}_\sigma & \mathbf{0} \\ \mathbf{0} & \mathbf{F}_\pi \end{pmatrix} \begin{pmatrix} \mathbf{C}_\sigma & \mathbf{0} \\ \mathbf{0} & \mathbf{C}_\pi \end{pmatrix} = \begin{pmatrix} \mathbf{S}_\sigma & \mathbf{0} \\ \mathbf{0} & \mathbf{S}_\pi \end{pmatrix} \begin{pmatrix} \mathbf{C}_\sigma & \mathbf{0} \\ \mathbf{0} & \mathbf{C}_\pi \end{pmatrix} \begin{pmatrix} \epsilon_\sigma & \mathbf{0} \\ \mathbf{0} & \epsilon_\pi \end{pmatrix} \quad (16)$$

Hückel theory is then concerned with the calculation of the  $\pi$ -MO-s only, by solving

$$\mathbf{F}_\pi \mathbf{C}_\pi = \mathbf{S}_\pi \mathbf{C}_\pi \epsilon_\pi. \quad (17)$$

2. The  $\pi$  basis set is assumed to be a minimal basis, consisting of atomic  $2p$  orbitals, one on each carbon atom. Assuming that the molecule is in the  $xy$  plane, its  $\pi$  MO-s are then constructed in terms of the set of  $2p_z$  AO-s of the carbon atoms.
3. All diagonal elements of the  $\pi$  Fock matrix are represented by a single parameter,  $\alpha$ , which represents the energy of an electron in a  $2p_z$  atomic orbital that includes its interaction with the rest of the molecule, according to the definition of a diagonal Fock matrix element. All off-diagonal elements between AO-s on neighbour, i.e. bonded atoms, are assigned a single parameter,  $\beta$ , which is assumed to be a negative quantity. All other off-diagonal Fock matrix elements are assumed to be negligible. The neglect of integrals between non-neighbour atoms is known as the *tight-binding approximation*, and, as Ruedenberg [26] pointed out, it is a justifiable first approximation, whereas “the outright neglect of neighbour overlap is not.” The Hückel (Fock) matrix is thus

$$\mathbf{F}_\pi = \alpha \mathbf{I} + \beta \mathbf{M} , \quad (18)$$

where  $\mathbf{I}$  is the unit matrix and  $\mathbf{M}$  is the topological or connectivity matrix which specifies the presence or absence of bonds between all pairs of atoms. For butadiene, for example, we have

$$\mathbf{M} = \begin{pmatrix} 0 & 1 & 0 & 0 \\ 1 & 0 & 1 & 0 \\ 0 & 1 & 0 & 1 \\ 0 & 0 & 1 & 0 \end{pmatrix} , \quad (19)$$

where the numbering of carbon atoms and hence of the  $2p_z$  atomic orbitals is sequential, starting at one end of the molecule.

4. In the simplest formulation of Hückel theory the  $2p_z$  atomic orbitals are assumed to be orthonormal. The Hückel  $\pi$ -MO equations are then simply

$$\mathbf{F}_\pi \mathbf{C}_\pi = \mathbf{C}_\pi \boldsymbol{\varepsilon}_\pi . \quad (20)$$

The corresponding eigenvalues are

$$\varepsilon_i = \alpha + \lambda_i \beta , \quad (21)$$

where the coefficients  $\{\lambda_i\}$  are eigenvalues of the topological matrix  $\mathbf{M}$ . We will refer to this approach as the *standard Hückel model*. We recall here, however, that the neglect of overlap between neighbour atoms is not a justifiable approximation according to Ruedenberg's analysis [26].

Since  $\beta$  is negative, the bonding, non-bonding and antibonding MO-s correspond to positive, zero and negative eigenvalues of  $\mathbf{M}$ , respectively. The energies of the MO-s directly correlate with the number of nodal planes. Thus, for butadiene the normalized MO-s and their energies are

$$(\psi_1 \quad \psi_2 \quad \psi_3 \quad \psi_4) = (\chi_1 \quad \chi_2 \quad \chi_3 \quad \chi_4) \begin{pmatrix} 0.37 & 0.60 & 0.60 & 0.37 \\ 0.60 & 0.37 & -0.37 & -0.60 \\ 0.60 & -0.37 & -0.37 & 0.60 \\ 0.37 & -0.60 & 0.60 & -0.37 \end{pmatrix} \quad (22)$$

$$\varepsilon_1 = \alpha + 1.62\beta, \quad \varepsilon_2 = \alpha + 0.62\beta, \quad \varepsilon_3 = \alpha - 0.62\beta, \quad \varepsilon_4 = \alpha - 1.62\beta . \quad (23)$$

For any given MO the presence of a nodal plane between two neighbour atoms is indicative of antibonding character between those particular atoms, as the node signifies destructive interference of the AO-s. For butadiene thus, occupancy of the second MO would weaken the  $\pi$ -bond between atoms 2 and 3, while strengthening those between atoms 1 and 2, as well as between 3 and 4. Such effects are given a quantitative measure by the first order reduced density matrix in the AO representation,  $\mathbf{D}$ , which in Hückel theory is generally known as the charge and bond order matrix. It is defined as

$$\mathbf{D} = \mathbf{C}_\pi \mathbf{n} \mathbf{C}_\pi^\dagger, \quad (24)$$

where  $\mathbf{n}$  is the diagonal MO occupancy matrix with elements 2, 1 or 0. The off-diagonal elements of  $\mathbf{D}$  are the bond orders, with values ranging from 0 to 1, where  $D_{pq} = 1$  signifies a conventional two-centre  $\pi$ -bond, as in ethylene. In butadiene the  $\pi$ -bond orders are 0.89, 0.45 and 0.89. Thus, Hückel theory predicts in a qualitatively correct manner that there is an alternation of  $\pi$ -bond strengths in conjugated polyenes which accounts for the observed variation of CC bond lengths. In fact, the Hückel-SCF model [27], in which the  $\beta$ -parameters are defined to be bond length dependent, while the bond lengths in turn are determined on the basis of the corresponding bond orders in a self-consistent way, has been found to be a useful and reliable computational approach in a number of applications [28-32].

As noted above, the most obvious discrepancy of the standard Hückel model is the neglect of the overlap integrals between the  $2p_z$  AO-s on neighbour atoms, i.e. atoms which are directly bonded to each other. This approximation actually introduces an inconsistency in that if such an approximation were justified, then  $\beta$  would also be negligible since the latter is overlap dependent. The justification, in the words of Coulson, is that “Historically, people have tended not to include it (overlap) because it turns out not to make much numerical difference” [33]. However, in the spirit of the Hückel parametrization, this problem is easily remedied, by approximating the overlap matrix  $\mathbf{S}$  as

$$\mathbf{S} = \mathbf{I} + \gamma \mathbf{M}, \quad (25)$$

where  $\gamma$ , a third Hückel parameter, is a measure of the average overlap integral between the  $2p_z$  AO-s on bonded atoms. Since  $\mathbf{F}_\pi$ ,  $\mathbf{M}$  and  $\mathbf{S}$  have a common set of eigenvectors,  $\mathbf{U}$ , i.e.,

$$\begin{aligned} \mathbf{S}\mathbf{U} &= (\mathbf{I} + \gamma \mathbf{M})\mathbf{U} = \mathbf{U}(\mathbf{I} + \gamma \boldsymbol{\epsilon}), \\ \mathbf{F}_\pi \mathbf{U} &= (\alpha \mathbf{I} + \beta \mathbf{M})\mathbf{U} = \mathbf{U}(\alpha \mathbf{I} + \beta \boldsymbol{\epsilon}), \end{aligned} \quad (26)$$

where  $\boldsymbol{\lambda}$  is the diagonal matrix of eigenvalues of  $\mathbf{M}$ . The eigenvalues,  $\boldsymbol{\epsilon}$ , and eigenvectors,  $\mathbf{C}_\pi$  of the generalized eigenvalue equations (17) are simply

$$\epsilon_i = \frac{\alpha + \beta \lambda_i}{1 + \gamma \lambda_i} \quad (27)$$

$$\mathbf{C}_\pi = \mathbf{U}(\mathbf{I} + \gamma \boldsymbol{\lambda})^{-1/2}. \quad (28)$$

This formalism, originally proposed by Wheland [34], will be referred to as the *standard Hückel model with overlap*. In comparison with the two-parameter standard model, the inclusion of differential overlap integrals results in higher energies, except for non-bonding MO-s whose energies would be unaffected. Thus, the bonding MO-s become less bonding, while the antibonding ones become more antibonding. The MO energy levels for butadiene obtained by the application of these two Hückel models are compared in Figure 10. An important consequence of the above parametrization is that the only change in the MO-s brought about by the introduction of explicit overlap is their renormalization, whereby all elements of the  $i$ -th column vector of  $\mathbf{U}$  are multiplied by a (re)-normalization constant of  $(1 + \gamma \lambda_i)^{-1/2}$ .

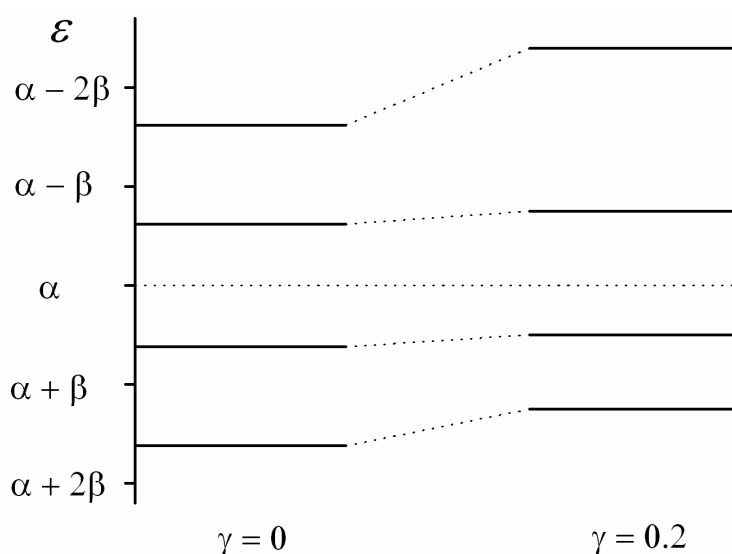


Fig. 10. Butadiene: Comparison of Hückel  $\pi$ -MO energy levels calculated by standard model ( $\gamma = 0$ ) and with the inclusion of overlap ( $\gamma = 0.2$ ), with  $\alpha = 0$ .

An alternative, implicit way of incorporating overlap in the Hückel model is to assume that the  $2p_z$  AO basis is a rigorously orthonormal basis,  $\{\phi_i\}$ , consisting of Löwdin orthogonalized AO-s [35]. The Löwdin process [36], known also as symmetric orthogonalization, is defined by the linear transformation

$$\phi = \chi S^{-1/2}. \quad (29)$$

This formalism, termed *Hückel model in OAO basis*, where the  $\alpha$  and  $\beta$  parameters of Hückel theory are defined with respect to the Löwdin orthogonalized  $2p_z$  AO basis, is formally equivalent to the standard (two-parameter) model developed above, but the interpretation of the parameters, especially from the point of view of chemical bonding is quite different, as discussed below.

### 5.1 The hydrogen molecule ion

The hydrogen molecule ion,  $H_2^+$ , is the textbook example of covalent chemical bonding as well as of the basic principle of molecular orbital (MO) theory. It also represents a natural starting point for Hückel theory. The simplest representation of the (normalized) bonding and antibonding wave functions,  $\psi_{\pm}$ , are in- and out-of-phase combinations of the 1s atomic orbitals (AO) of hydrogen,  $\chi_a, \chi_b$ , centred on the nuclei  $a$  and  $b$  (with a fixed orbital exponent  $\zeta = 1$ ):

$$\psi_{\pm} = [2(1 \pm S_{ab})]^{-1/2} (\chi_a \pm \chi_b), \quad (30)$$

where  $S_{ab}$  is the overlap matrix element of the two AO-s. The corresponding energies (in atomic units) in terms of overlap ( $S$ ), kinetic ( $T$ ) and nuclear attraction ( $V$ ) integrals are

$$E_{\pm} = \frac{(T_{aa} \pm T_{ab}) + (V_{aa} \pm V_{ab})}{(1 \pm S_{ab})} + \frac{1}{R} \quad (31)$$

where the last term is the nuclear repulsion energy at an arbitrary internuclear distance  $R$ . Thus the interaction between the AO-s is quantified by the three coupling matrix elements

$$S_{ab} = \langle \chi_a | \chi_b \rangle, \quad T_{ab} = \langle \chi_a | \hat{T} | \chi_b \rangle, \quad V_{ab} = \langle \chi_a | \hat{V} | \chi_b \rangle, \quad (32)$$

where  $\hat{V}$  represents the attractive Coulomb potential of both nuclei. The resulting total energies  $E_{\pm}$  as a function of the bond length are shown in Figure 11.

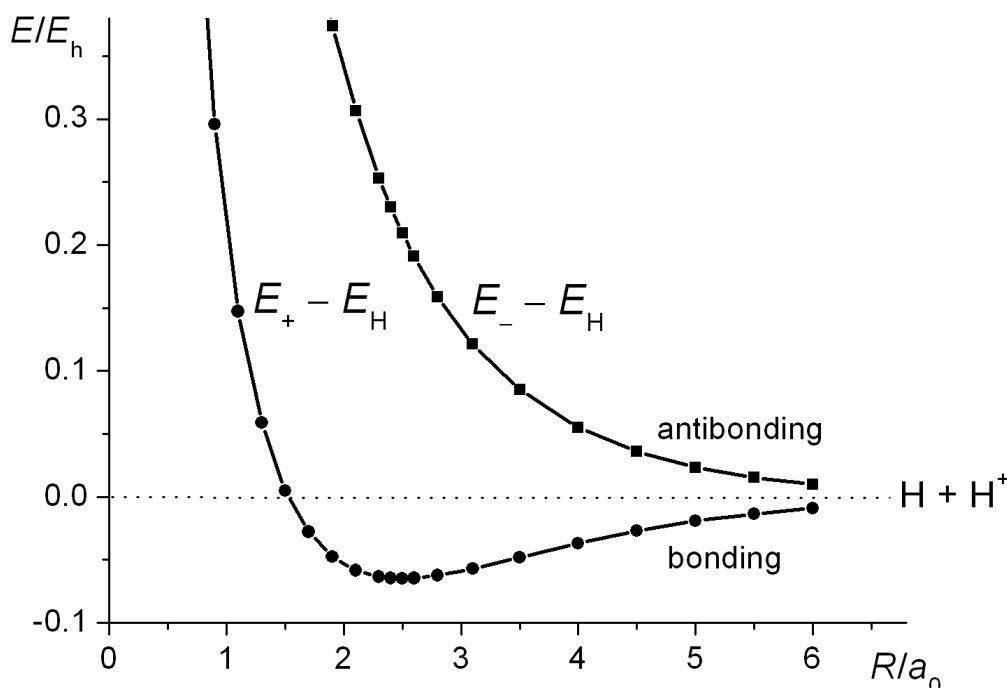


Fig. 11.  $H_2^+$  bonding and antibonding potential energy curves calculated using 1s AO-s with a fixed orbital exponent of 1.

The calculation predicts the existence of a stable molecule with an equilibrium bond length of  $2.5 a_0$  and a dissociation ( $D_e$ ) or bond energy of  $0.0648 E_h$ , i.e.  $170 \text{ kJ mol}^{-1}$ . The experimental values are  $2.0 a_0$  and  $270 \text{ kJ mol}^{-1}$ . Thus this simplest of MO calculations yields results that are qualitatively correct.

While non-zero overlap is manifested in non-zero kinetic and potential interactions between the AO-s, it also gives rise to a direct energetic effect known as Pauli repulsion. So as to separate the effect of the latter from the direct kinetic and potential components of the bond energy we orthogonalize the AO-s by Löwdin's symmetric orthogonalization method, as discussed in the previous section. The resulting OAO-s have the property that they resemble the original atom-centred AO-s to the maximum degree, i.e. the dominant contribution to each OAO is from a specific AO. In the present case of  $H_2^+$ , the normalized OAO-s are

$$\begin{aligned} \phi_1 &= N(\chi_1 - \mu\chi_2), \\ \phi_2 &= N(\chi_2 - \mu\chi_1), \end{aligned} \quad (33)$$

where the constants  $\mu (<1)$  and  $N$  can be shown to be



$$\mu = \frac{1 - (1 - S_{12}^2)^{1/2}}{S_{12}}, \quad (34)$$

$$N = (1 - 2\mu S_{12} + \mu^2)^{-1/2}. \quad (35)$$

Since  $N \geq 1$ , the orthogonalization process results in increased density close to the centre of the dominant AO which is compensated by a reduction in density in the nodal region of the OAO.

An important aspect of the orthogonalization procedure is the behaviour of the kinetic energy matrix elements. In the AO basis the diagonal elements are large and positive, while the off-diagonal elements are at least an order of magnitude smaller. With regard to the latter, it is instructive to rewrite such a quantity as

$$\langle f | \hat{T} | g \rangle = \frac{\hbar^2}{2m} \int_{-\infty}^{\infty} d\mathbf{r} \nabla f(\mathbf{r}) \cdot \nabla g(\mathbf{r}) \quad (36)$$

where  $\hbar = h/2\pi$ ,  $h$  being Planck's constant, and  $m$  is the electronic mass. According to the above equation (obtained via integration by parts) the sign of the kinetic matrix element is determined by the relative signs of the gradients of the wave functions  $f$  and  $g$  in the overlap region. In the case of two AO-s on different atoms the signs of the bond-perpendicular gradients of the two AO-s are the same, but would be different for the bond-parallel components for all reasonable bond distances. Hence an off-diagonal kinetic energy matrix element would consist of a negative bond-parallel component and a positive bond-perpendicular component.

The kinetic energy matrix elements obtained from the above  $\text{H}_2^+$  calculations are shown in Figure 12. We note that as the molecule forms, i.e. the internuclear distance decreases, the effect of Löwdin orthogonalization is to increase the diagonal kinetic energy elements but decrease the off-diagonal elements to negative values. The former effect is the increasing Pauli repulsion with increasing overlap, while the latter represents the energetic stabilization associated with electron delocalization, i.e. covalent bond formation.

The effect of Löwdin orthogonalization on the potential energy (nuclear attraction) matrix elements is quite different, as shown in Figure 13. In the OAO basis the coupling matrix element  $V_{ab}$  is near-zero at all distances, while  $V_{aa}$  varies inversely with the kinetic term  $T_{aa}$ . In fact the sum  $T_{aa} + V_{aa}$  is largely constant throughout the range of bond lengths: it varies between  $-0.698 E_h$  at  $R = 5 a_0$  and  $-0.871 E_h$  at  $R = 1 a_0$ .

The total energy, when expressed in terms of the OAO matrix elements, is simply

$$E_+ = [T_{aa} + V_{aa} + V_{ab} + 1/R] + T_{ab}. \quad (37)$$

Noting that the sum of the bracketed terms monotonically increases with decreasing bond distance, it follows that the equilibrium binding, which occurs in the region of  $2.5 a_0$ , is entirely due to the contribution of the coupling kinetic energy matrix element  $T_{ab}$  to the energy. The conclusion that follows is well known, inasmuch as an MO calculation using a fixed exponent minimal basis predicts that covalent bonding is due to a drop in the kinetic

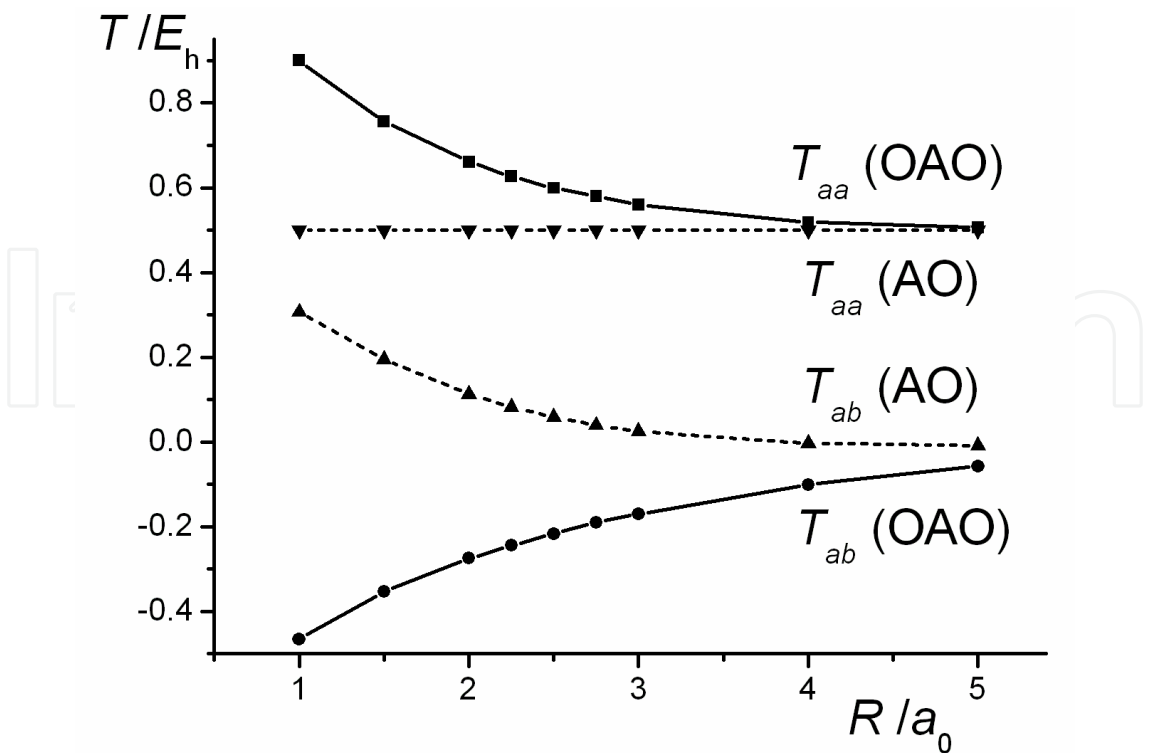


Fig. 12. Kinetic energy matrix elements for  $H_2^+$  with respect to (non-orthogonal) 1s AO-s and Löwdin OAO-s.

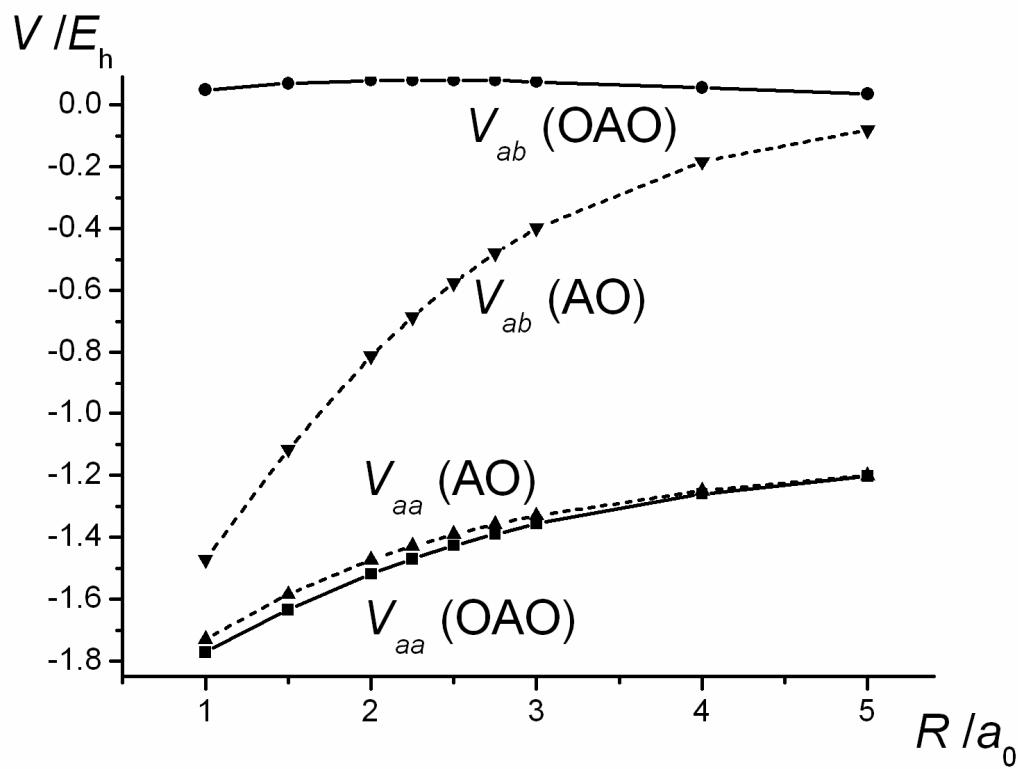


Fig. 13. Potential energy (nuclear attraction) matrix elements for  $H_2^+$  with respect to (non-orthogonal) 1s AO-s and Löwdin OAO-s.

energy as the molecule's constituent atoms come together. The same conclusions apply in the more general case of optimised exponents, provided we allow for orbital contraction, as pointed out by Ruedenberg.

To provide more insight into the mathematical reasons for these changes consider the diagonal and off-diagonal matrix elements of the (Hermitean) kinetic energy operator  $\hat{T}$  that arise when two real orbitals are Löwdin orthogonalized, as described above. The transformed matrix elements are

$$\begin{aligned}\langle \phi_1 | \hat{T} | \phi_1 \rangle &= N^2 \left( \langle \chi_1 | \hat{T} | \chi_1 \rangle + \mu^2 \langle \chi_2 | \hat{T} | \chi_2 \rangle - 2\mu \langle \chi_1 | \hat{T} | \chi_2 \rangle \right) \\ &\approx N^2 \langle \chi_1 | \hat{T} | \chi_1 \rangle > \langle \chi_1 | \hat{T} | \chi_1 \rangle\end{aligned}\quad (38)$$

$$\begin{aligned}\langle \phi_1 | \hat{T} | \phi_2 \rangle &= N^2 \left( -\mu \langle \chi_1 | \hat{T} | \chi_1 \rangle - \mu \langle \chi_2 | \hat{T} | \chi_2 \rangle + (1 + \mu^2) \langle \chi_1 | \hat{T} | \chi_2 \rangle \right) \\ &\approx -2N^2 \mu \langle \chi_1 | \hat{T} | \chi_1 \rangle < 0.\end{aligned}\quad (39)$$

Using the overlap and kinetic energy matrix elements computed for  $\text{H}_2^+$  at a range of distances we find that in both expressions the terms involving the diagonal matrix elements, i.e.  $\langle \chi_1 | \hat{T} | \chi_1 \rangle$  and  $\langle \chi_2 | \hat{T} | \chi_2 \rangle$ , are dominant. (The same pattern has been found for the  $p_\pi$  orbitals of ethylene and benzene, computed at the SCF/STO-3G level of theory, to be discussed later.) The net result is that the kinetic energy of an OAO is larger than that for the AO, and the off-diagonal kinetic energy matrix element between two OAO-s is negative, as noted above. The physical explanation for the increased kinetic energy content, in the words of Weber and Thiel [37], is that "the orthogonalization accounts for the Pauli repulsion of the electrons at other centres and prevents penetration into these regions, thus effectively reducing the volume for an electron in the OAO and increasing its kinetic energy". In the case of Löwdin orthogonalized AO-s the dominant contributions arise from the regions where the dominant component of a given OAO interacts with the "orthogonalization tail" of the other, and where the gradients of the OAO-s with respect to all coordinates differ in sign.

In the context of Hückel MO theory, we note that the energy of  $\text{H}_2^+$  at any distance can be written in terms of distance dependent  $\alpha$  and  $\beta$  parameters:

$$E_+(R) = \alpha(R) + \beta(R) + 1/R, \quad (40)$$

where

$$\alpha(R) = T_{aa}(R) + V_{aa}(R) \quad (41)$$

and

$$\beta(R) = T_{ab}(R) + V_{ab}(R), \quad (42)$$

where the matrix elements are evaluated in the OAO basis. While similar, but more complex expressions can be easily derived for the *standard Hückel model with overlap*, the inherent simplicity of the former makes it more attractive. More importantly, however, in the *Hückel model in OAO basis*, the Pauli repulsion is rigorously separated from the effects of delocalization and covalent bonding. In other words, use of OAO bases represents a natural starting point for the analysis and ultimately the understanding of covalent bonding.

## 5.2 The ethylene molecule

Ethylene is the classic  $\pi$ -bonded molecule which often serves as the starting point for the parametrization of Hückel MO theory. The bonding and antibonding  $\pi$  MO-s of ethylene are formally the same as the  $\sigma$  MO-s of  $H_2^+$ , but there are two important differences: (1)  $\pi$  MO-s are constructed from  $p_z$ -type MO-s which are parallel to each other, hence their interaction matrix elements are in general smaller than those of  $s$  and  $p$  AO-s in head to head arrangements. (2) In a many-electron molecule such as ethylene the potential energy of a given electron includes its interaction with all other electrons, as well as the field due to the nuclei, as implemented in the SCF process.

Computed values of the kinetic and potential matrix elements of the  $2p_z$  AO-s and OAO-s are shown for a range of C-C distances in Figures 14 and 15. The CH distances and bond angles are fixed at their experimental values. The matrix elements were calculated from SCF/STO-3G kinetic energy and Fock matrix elements of ethylene. The potential energy matrix elements are simply

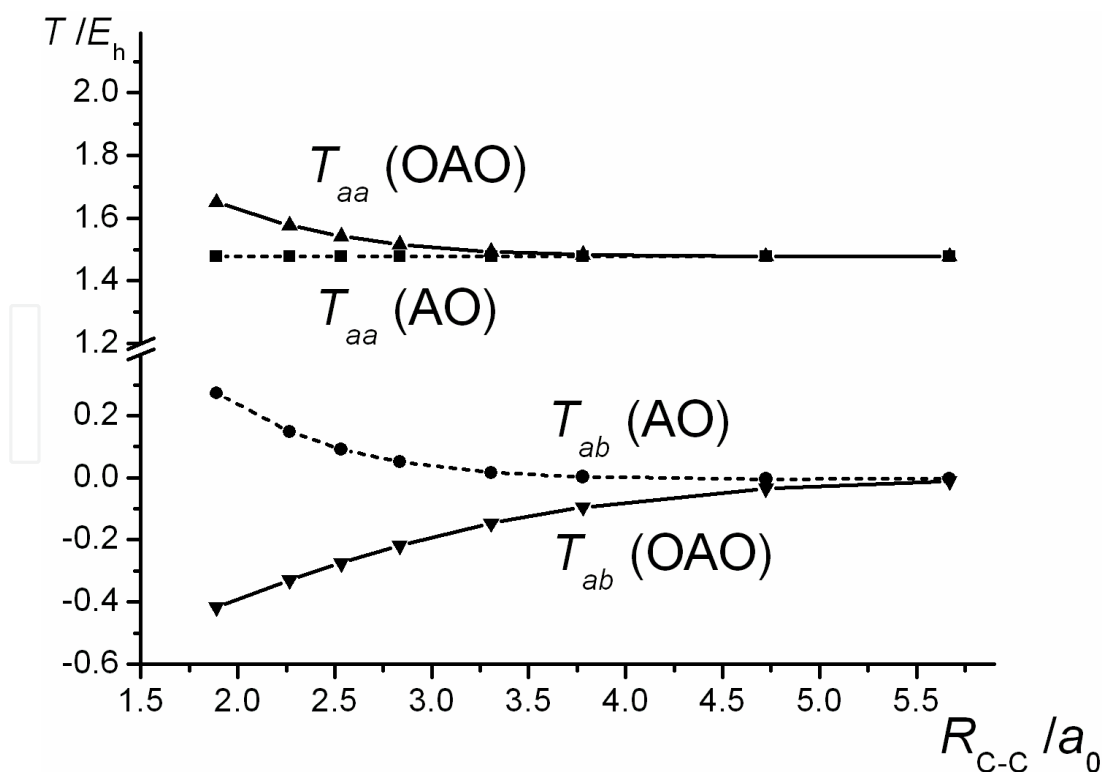


Fig. 14. Kinetic energy matrix elements for  $2p_z$  orbitals of ethylene with respect to (non-orthogonal) AO-s and Löwdin OAO-s.

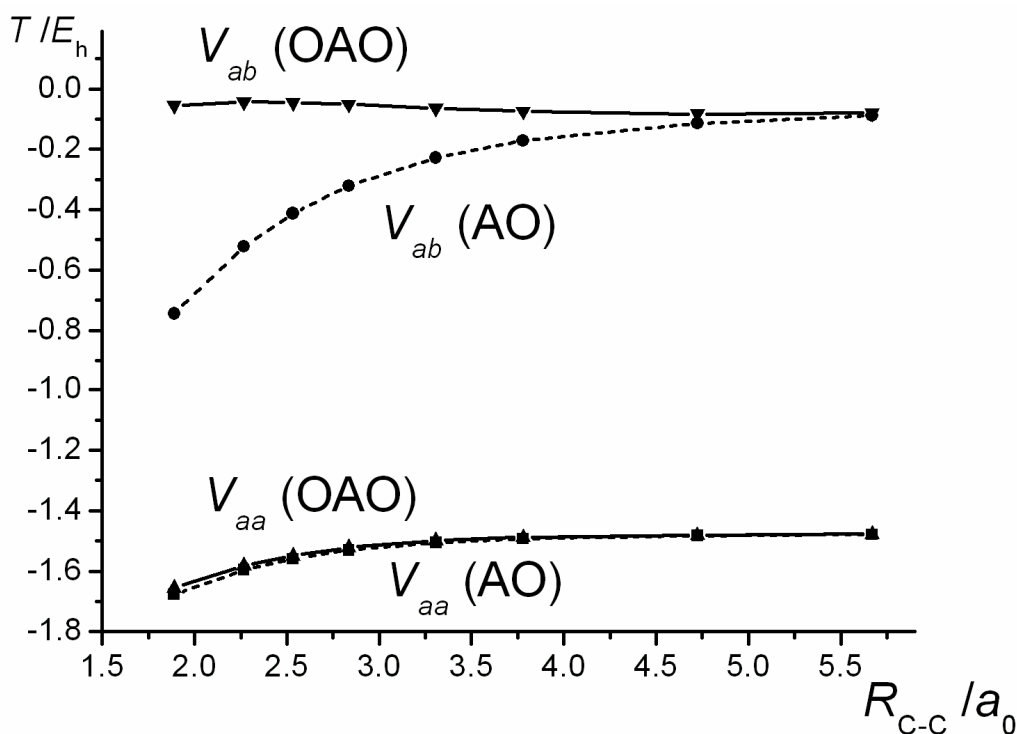


Fig. 15. Potential energy matrix elements for  $2p_z$  orbitals of ethylene with respect to (non-orthogonal) AO-s and Löwdin OAO-s.

$$V_{ij} = F_{ij} - T_{ij}, \quad i, j = a, b. \quad (43)$$

where  $F_{ij}$  is the Fock matrix element between AO-s  $i, j$ .

The C-C distance dependence of these matrix elements is qualitatively the same as what was obtained for  $H_2^+$  (Figures 12 and 13). Consequently the same observations and conclusions apply for the formation of a simple  $\pi$ -bond in ethylene as for the  $\sigma$ -bond in  $H_2^+$ . Thus, in the OAO representation  $\pi$ -bonding is the result of the negative kinetic interaction between the two OAO-s. As the  $\pi$  MO-s are eigenfunctions of the  $\pi$  block of the Fock matrix (see equation (10)), the Hückel parameters can readily be identified as the appropriate Fock matrix elements of a minimal basis computation, i.e.

$$\alpha = F_{aa}, \quad \beta = F_{ab}. \quad (44)$$

The  $\pi$  orbital energies of ethylene as a function of the C-C distance, as obtained in the current SCF/STO-3G calculations, are given in Figure 16. As expected, the splitting of the bonding and antibonding energies is strongly dependent on the interatomic distance. This is a consequence of the distance dependence of the kinetic energy matrix element  $T_{ab}$ , which in turn determines the behaviour of the Fock matrix element  $F_{ab}$ , i.e.  $\beta$  of Hückel theory. The kinetic energies (relative to that of a  $2p_z$  AO) of the bonding  $\pi$  and antibonding  $\pi^*$  MO-s are also shown in Figure 16. Clearly, the distance dependence of the MO-s is determined by their kinetic energy content.

We conclude this section with the observation that the Hückel description of  $\pi$ -bonding in ethylene is exactly the same as that of the covalent bond in  $H_2^+$ . In both molecules the

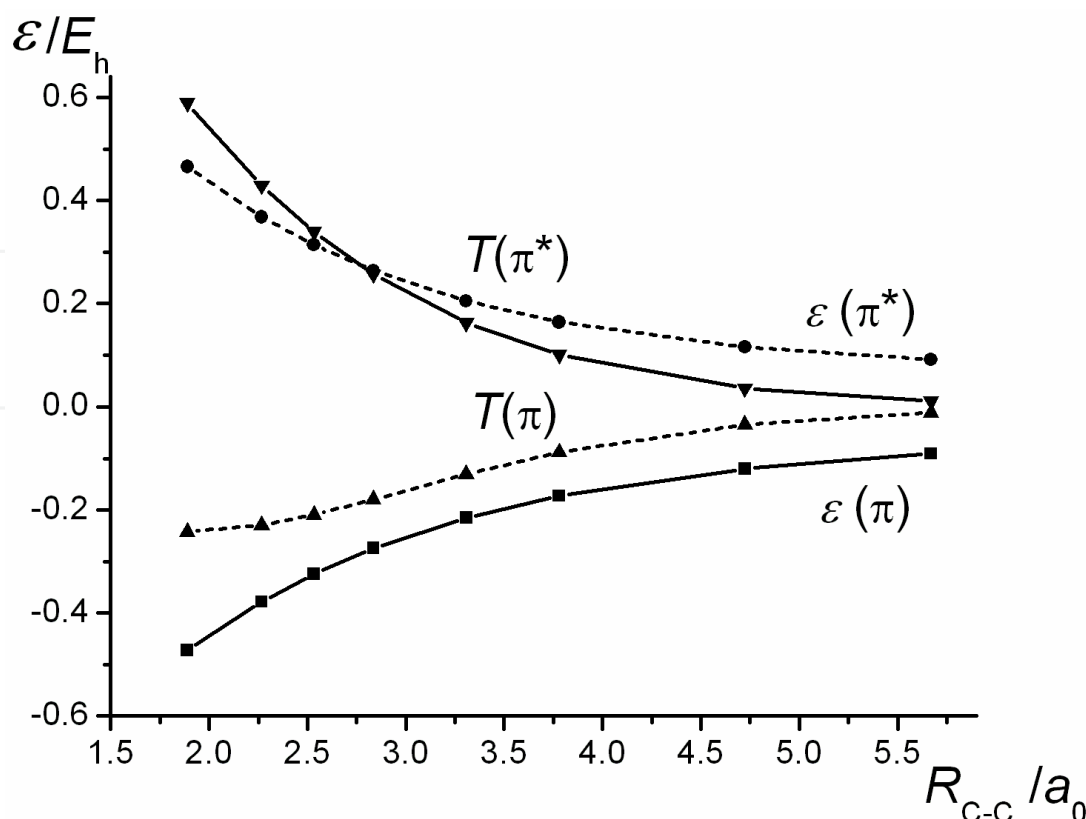


Fig. 16. Total orbital and kinetic energies of the bonding  $\pi$  and antibonding  $\pi^*$  MO-s of ethylene computed at the SCF/STO-3G level of theory. The kinetic energies are relative to that of a  $2p_z$  AO ( $1.4777 E_h$ ).

bonding and antibonding energy levels can be determined in terms of the Hückel  $\alpha$  and  $\beta$  parameters, where  $\alpha$  represents the energy of an electron in an OAO and  $\beta$  is the coupling matrix element between the OAO-s on the bonded atoms of the molecule.  $\beta$  is negative and predominantly kinetic in character. Thus for the bonding MO, which is the in-phase combination of the OAO-s, the energy stabilization relative to the OAO-s is due to delocalization and the concomitant drop in kinetic energy. The opposite holds for the antibonding MO, the out-of-phase combination of OAO-s, where the energetic destabilization is due to the presence of the extra node in the MO.

### 5.3 Benzene

In conjugated molecules there is an extra degree of stabilization of the bonding MO-s due to the extra degree of possible  $\pi$  delocalization. To further test the performance of the above Hückel models with regard to describing and interpreting  $\pi$ -bonding in planar conjugated hydrocarbons, we decided to parametrize the Hückel models on the basis of an ab initio minimal basis (STO-3G) Hartree-Fock calculation on benzene at its experimental equilibrium geometry. The high ( $D_{6h}$ ) molecular symmetry is evident in the overlap and Fock matrices; there are only four distinct type of elements in each, as indicated in Table 1, which lists the converged Fock, overlap and kinetic energy matrix elements in the  $2p_z$  AO basis and also in the Löwdin orthogonalized (OAO) basis. The in-plane ( $x,y$ ) components of the kinetic energy matrix elements are also shown (as  $T_{||}$ ).



$i,j$	AO				OAO		
	$S$	$F$	$T$	$T_{  }$	$F$	$T$	$T_{  }$
1,1; 2,2; 3,3;...	1.000	−0.103	1.478	0.296	0.004	1.590	0.362
1,2; 2,3; 3,4;...	0.214	−0.254	0.075	−0.081	−0.251	−0.263	−0.157
1,3; 2,4; 3,5;...	0.026	−0.041	0.000	−0.018	0.010	0.017	0.010
1,4; 2,5; 3,6;...	0.010	0.014	−0.004	−0.009	0.023	−0.013	−0.008

Table 1. Benzene: Overlap, Fock and kinetic energy matrix elements (in  $E_h$ ) in AO and OAO bases from ab initio (HF/STO-3G) calculations. (The orbitals are numbered sequentially around the ring.)

First, we note that the Hückel approximation, whereby off-diagonal overlap and Fock matrix elements between orbitals on atoms which are not directly bonded to each other (as listed in the last two rows of Table 1) are neglected, is justified. Secondly, however, the differential overlaps, i.e.  $S_{12}$ ,  $S_{23}$ ,...can hardly be judged as negligible. Thirdly, the orthogonalization has resulted in diagonal Fock matrix elements that are uniformly higher in energy, as expected, since the orthogonalization results in orbital contraction as well as delocalization by virtue of the “orthogonalization tails” possessed by the OAO-s. As discussed earlier in the section on  $H_2^+$ , an off-diagonal kinetic energy matrix element would consist of a negative bond-parallel component,  $T_{||}$ , and a positive bond-perpendicular component,  $T_{\perp}$ . In the case of benzene the former is actually the in-plane component. In the case of non-orthogonal AO-s the two components are positive and negative. As expected, Löwdin orthogonalization increases the diagonal elements of the kinetic energy matrix by  $\sim 0.11 E_h$ , but decreases both bond-parallel and bond-perpendicular components of the off-diagonal elements to large negative values.

As the data in Table 1 indicate, in the (non-orthogonal) AO basis the Fock matrix elements, in particular the off-diagonal elements,  $F_{12}$ ,  $F_{23}$ ,...are dominated by potential energy contributions. However, the large and definitely non-negligible overlap integrals,  $S_{12}$ ,  $S_{13}$ ,...are indicative of substantial Pauli repulsion, so that in the OAO basis the off-diagonal Fock matrix elements are almost entirely kinetic in character. Moreover, the increase in the diagonal Fock matrix elements brought about by the orthogonalization process is largely due to the analogous increase in the diagonal kinetic energy matrix elements.

Another notable consequence of the orthogonalization procedure is the decrease, by approximately a factor of 4, in the magnitude of the Fock matrix elements between AO-s on next nearest neighbouring atoms, viz. 1,3; 2,4; 3,5;... elements.

Utilizing the appropriate ab initio Fock and overlap matrix elements of benzene we can parametrize the three Hückel models as follows:

1. Standard Hückel model:

$$\alpha = F_{11} = F_{22} = \dots = -0.103 E_h$$
$$\beta = F_{12} = F_{23} = \dots = -0.254 E_h$$
$$\gamma = 0 .$$

(45)

2. Standard Hückel model with overlap: In addition to  $\alpha$  and  $\beta$ , as chosen for the standard model,

$$\gamma = S_{12} = S_{23} = \dots = 0.214 \quad (46)$$

3. Hückel model in OAO basis:

$$\alpha = F_{11}^{\text{OAO}} = F_{22}^{\text{OAO}} = \dots = 0.004 E_h \quad (47)$$

$$\beta = F_{12}^{\text{OAO}} = F_{23}^{\text{OAO}} = \dots = -0.251 E_h$$

Applying these three models to benzene, the energy levels obtained are shown in Figure 17, along with the *ab initio* SCF energies for comparison.

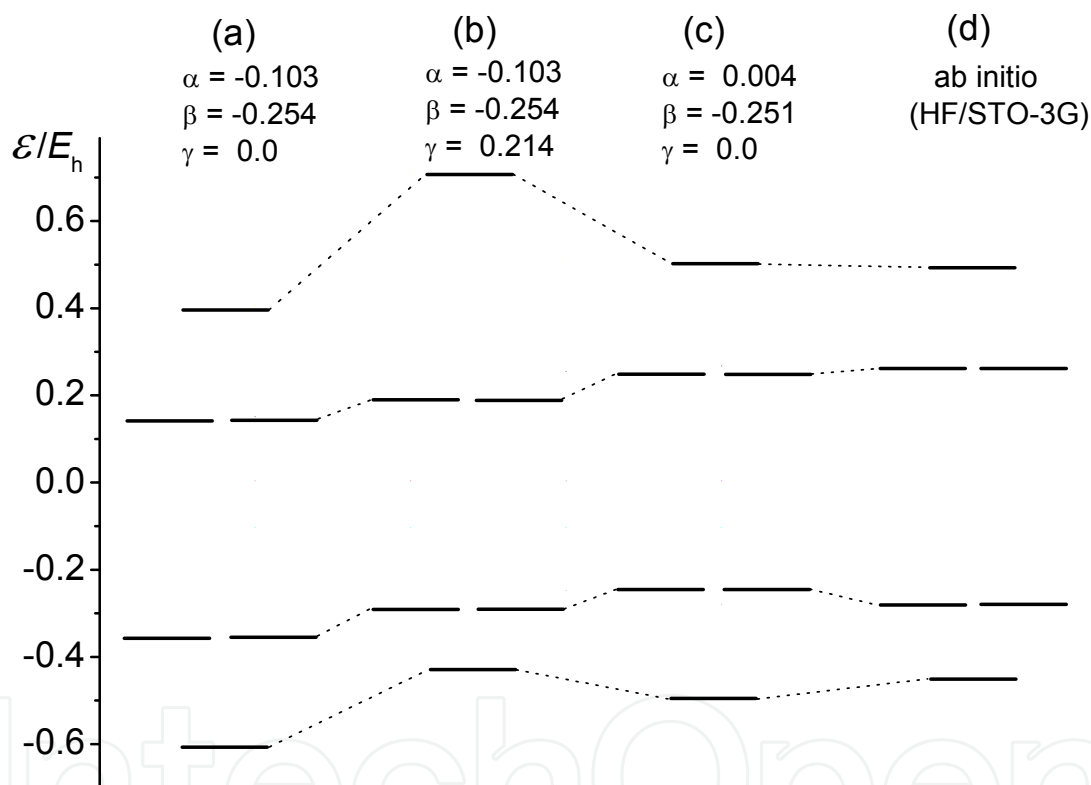


Fig. 17. Benzene: Comparison of  $\pi$  MO energy levels calculated by (a) standard Hückel model (b) standard Hückel model with overlap (c) Hückel model in OAO basis and (d) *ab initio* (HF/STO-3G) method.

The energy levels calculated by the standard model are uniformly too low in comparison with the *ab initio* values. This is attributable largely to the neglect of the differential overlap integrals. Their inclusion, according to the standard model with overlap, results in significant improvements in the energies of the bonding MO-s, but also an overcorrection to the energy of the highest antibonding MO. The best overall agreement with the *ab initio* results is obtained by the Hückel model in the OAO basis. The energies calculated by the latter approach are essentially the same as those from the standard model calculations plus a positive shift of  $\sim 0.1 E_h$ , since the respective  $\beta$  parameters are nearly the same.

Despite its simplicity, the standard model with overlap has not gained much popularity, largely because most workers in the field, especially prior to the development of more sophisticated semi-empirical and indeed *ab initio* methods, found that the standard model works well without the explicit allowance for overlap, as noted for example by Coulson [33]. It was also appreciated that the standard model can be regarded as being formally equivalent to the Hückel model in OAO basis, i.e. the neglect of overlap is rigorously justifiable [35]. Depending on the problem at hand, be it the estimation and/or rationalisation of stabilities in terms of  $\pi$ -delocalization, or the interpretation of electronic spectra, the  $\alpha$  and  $\beta$  parameters of Hückel theory are treated as adjustable empirical parameters, chosen so as to best fit experimental data. As remarked above, choosing  $\alpha$  and  $\beta$  to best model *ab initio* minimal basis SCF MO-s and their energies is a pedagogical exercise - we do not suggest that such a procedure is superior or preferable to the accepted practice when it comes to “real” applications. The difference between the two models arises, of course, in the computation of the MO coefficients. Use of the OAO basis implies that the MO-s are

$$\psi = \chi S^{-1/2} \mathbf{U}$$

(48)

where  $\mathbf{U}$  is the matrix of eigenvectors of the of the topology matrix,  $\mathbf{M}$ .

As a further test of the three Hückel models for benzene, the kinetic and potential energy components of the computed orbital energies are listed in Table 2, where each MO is labelled by the number of its nodal planes.

Number of nodes	$\varepsilon$				$\langle T \rangle$				$-\langle V \rangle$			
	1	2	3	4	1	2	3	4	1	2	3	4
Standard Hückel	−0.61	−0.36	0.15	0.41	1.63	1.55	1.40	1.33	2.24	1.91	1.25	0.92
Hückel with overlap	−0.43	−0.29	0.19	0.71	1.14	1.28	1.79	2.33	1.57	1.57	1.59	1.61
Hückel in OAO basis	−0.50	−0.25	−0.26	0.51	1.06	1.33	1.85	2.12	1.56	1.57	1.60	1.61
ab initio (HF/STO- 3G)	−0.46	−0.28	0.27	0.50	1.08	1.32	1.82	2.16	1.54	1.60	1.55	1.66
ab initio $\langle T_{  } \rangle$					0.06	0.20	0.50	0.70				

Table 2. Benzene: Total orbital energies of Hückel and ab initio MO-s and their kinetic and potential energy components (in  $E_h$ ).

The two Hückel models, which include overlap, reproduce the ab initio kinetic and potential orbital energies quite accurately, providing further support for the view that these models

capture the essential features of the more sophisticated *ab initio* approach to MO theory. Neglecting differential overlap integrals, as invoked in the standard model, yields qualitatively different results: the ordering of the MO-s in the standard model is determined by the potential energy, as the apparent kinetic energies of the MO-s depend *inversely* on the number of nodes, due to the neglect of Pauli repulsion. To help with our understanding of these effects consider the kinetic energy associated with a given MO, as obtained from equation (27):

$$\langle T \rangle = \frac{\langle \psi_i | \hat{T} | \psi_i \rangle}{\langle \psi_i | \psi_i \rangle} = \frac{\alpha_T + \lambda_i \beta_T}{1 + \lambda_i \gamma} \quad (49)$$

where  $\alpha_T$  and  $\beta_T$  are the kinetic energy components of  $\alpha$  and  $\beta$  respectively. As noted already, in the standard model the kinetic energy contributions to the  $\beta$  parameters, although effectively negligible, are actually positive. The variation in kinetic energy among the MO-s is largely determined by the variation in energy denominators which depend inversely on the eigenvalues,  $\{\lambda_i\}$ , which in turn are in a direct relationship with the total energies,  $\{\varepsilon_i\}$ . However, in the absence of Pauli repulsion, i.e. overlap effects, the kinetic energy of the  $i$ -th MO would be determined by the energy numerator  $\alpha_T + \lambda_i \beta_T$  alone, which gives rise to the incorrect nodal dependence of the kinetic energy.

The apparent non-physical behaviour of the MO energies is a basic flaw of the standard Hückel model. It is caused by the inconsistency which is implicit in the formalism, i.e. the neglect of differential overlap in the parametrization of the overlap matrix, but *not* in the parametrization of the Fock matrix. We believe that from a pedagogical point of view we should not advocate this model as a qualitatively correct representation of the electronic structure of conjugated  $\pi$ -electron molecules, but rather as the first step in the development of an acceptable, i.e. physically correct, theory.

The above results graphically illustrate the importance of overlap integrals in the calculation of molecular wave functions and energies as well as in the description and interpretation of chemical bonding. Overlap integrals make an important contribution to the quantum mechanical coupling of (non-orthogonal) AO-s and, more generally, of atom-centred basis functions. Their neglect, as in the standard Hückel model, results in MO-s and energetics which would provide an incorrect interpretation of covalent bonding in terms of kinetic and potential energies. With the help of judiciously chosen empirical or semi-empirical parameters such overlap effects can be “folded” into those parameters in a range of popular semi-empirical methods which neglect differential overlap, although ultimately, as shown by the work of Weber and Thiel [37], significant improvements in accuracy and reliability can be achieved by the direct incorporation of overlap into these models. In the case of Hückel MO theory this can be achieved simply by adopting the OAO representation.

The interpretation of covalent bonding via the Hückel theory is particularly transparent by utilizing the model in OAO representation, as the role of kinetic energy and its origins in the context of bonding can be clearly seen. Löwdin orthogonalization of the AO-s accounts for the presence of Pauli repulsion between electrons in the AO-s and results, most significantly, in the contraction of the AO-s. The coupling between the resulting OAO-s is, however, very strong, negative and predominantly kinetic in character. Electronic

delocalization, as described by the formation of bonding MO-s, leads to stabilization, largely because of the concomitant drop in the kinetic energy. This is graphically illustrated by the results for benzene which are summarized in Figure 18, where the kinetic and potential energies of the MO-s are plotted against their total energies.

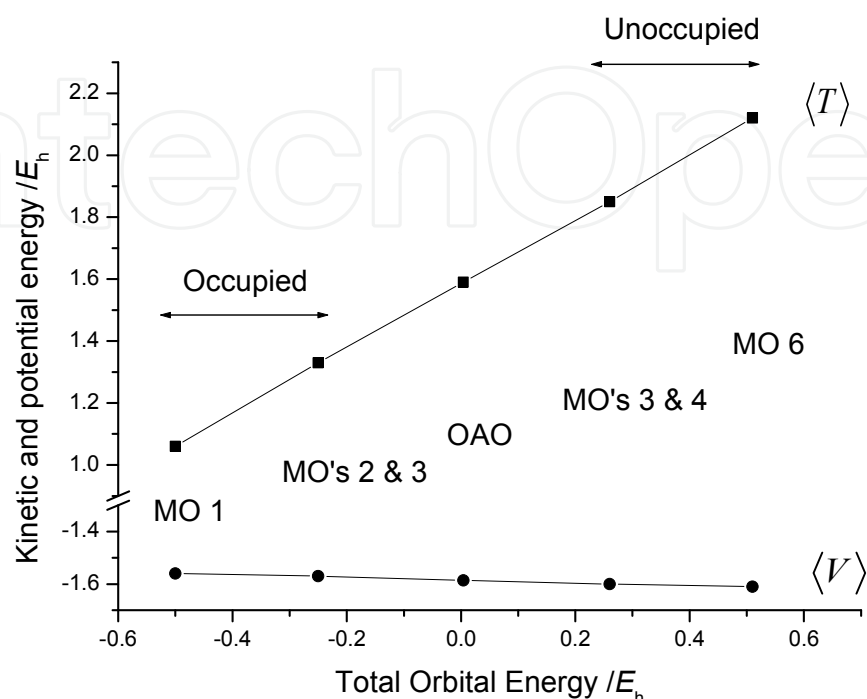


Fig. 18. Kinetic and potential energies  $\pi$ -MO-s and OAO-s of benzene as obtained by Hückel model in OAO basis.

The energetic stabilization and destabilization of the occupied and unoccupied MO-s (relative to an OAO) are clearly a consequence of the kinetic energy content of the MO-s. There is negligible variation in the potential energies of the MO-s. This picture is essentially the same as the description of Ruedenberg and co-workers [13, 38-41].

In summary, we note that, despite its apparent simplicity of application, the Hückel model clearly contains all the necessary quantum mechanical elements to describe  $\pi$ -bonding in polyenes. It enables us to interpret covalent bonding in a manner that is physically correct as well as transparent. It relies on just three parameters:  $\alpha$ , representing the binding of a  $\pi$ -electron occupying a  $2p_z$  AO to an atom;  $\beta$ , representing the quantum mechanical interaction between AO-s on neighbour atoms; and  $\gamma$ , which is the overlap between the coupled AO-s.  $\beta$  and  $\gamma$  can be thought of as two sides of the same coin, as both are crucial in the correct description of the coupling between two AO-s. By reformulating the Hückel model in terms of a Löwdin orthogonalized AO basis, the number of parameters is reduced, as only  $\alpha$  and  $\beta$  need to be defined. Solution of the Hückel equation results in delocalized MO-s with a range of energies which are lower as well as higher than  $\alpha$ , depending on the number of nodes in the MO-s and on the magnitudes of  $\beta$  and  $\gamma$ .

The degree of  $\pi$ -bonding, i.e.  $\pi$  stabilization, that occurs in a given molecule is determined by the overall accumulated contributions of the  $\beta$  coupling terms resulting from the appropriate occupancy of the lowest energy MO-s. It will be argued in a later section, that

Hückel MO-s are maximally delocalized, and therefore they naturally provide an optimal description of  $\pi$ -bonding, since the degree of delocalization is a key factor that effectively governs the degree of stabilization. An important point that emerges from this analysis is that the mechanism of binding an electron within an atom, as represented by  $\alpha$  is of no consequence. All that is needed is an attractive atomic potential. In other words, the particular form of the Coulomb attraction that binds electrons does not play a crucial role in the covalent bonding mechanism. The latter depends on delocalization and quantum mechanical coupling of (localized) AO-s and is not affected by the exact nature of the inter-particle forces.

#### 5.4 Extensions of Hückel Theory

Hückel MO theory in its standard form describes the  $\pi$ -electron structure of conjugated polyenes. It can be, as indeed it has been, generalized in a number of ways so as to be applicable e.g. to  $\pi$  systems with heteroatoms, the treatment of  $\sigma$ -bonding – as we have done above – and the description of solids.

The generalized Hückel method, more widely known as the Pariser-Parr-Pople (PPP) method [42-45] is a semi-empirical  $\pi$ -MO theory, where electron repulsion effects are explicitly, although approximately, allowed for. PPP utilizes the tight binding approximation and it is parametrized in terms of one- and two-electron integrals chosen largely on the basis of experimental data.

The extended Hückel MO (EHMO) method, developed by Hoffmann [46], is a valence MO theory, i.e.  $\sigma$ - and  $\pi$ -electrons are treated on equal footing. The diagonal Fock matrix elements,  $\{F_{ii}\}$  (in a minimal basis) are parametrized on the basis of atomic ionization energies, while the off-diagonal elements,  $\{F_{ij}\}$ , following the recommendation of Wolfsberg and Helmholz [47], are specified simply as

$$F_{ij} = KS_{ij}(F_{ii} + F_{jj})/2, \quad (50)$$

where  $S_{ij}$  is an overlap integral computed in a minimal Slater orbital basis and  $K$  is an adjustable parameter, usually  $\sim 1.75$ . The MO-s and their energies are obtained by solving the generalized eigenvalue equations (13); the total molecular energy is simply defined as the sum of the occupied MO energies. As the overlap integrals are computed at any given molecular geometry (rather than parametrized), the EHMO method allows geometry optimizations to be carried out.

Basic Hückel theory lies at the heart of the widely used tight binding method of material modelling [48]. The formalism was first developed by Slater and Koster [49] in an attempt to generalize the LCAO method to infinite periodic crystals by means of Bloch sums. The AO basis in a tight binding calculation is understood to be a Löwdin orthonormalized basis. The Hamiltonian, i.e. Fock matrix elements, are formally defined with respect to the orthogonal AO basis, although it is generally parametrized, such that, e.g. the two-centre integrals are represented by parameters that depend on the distance between the atomic centres, rather like in Hoffmann's EHMO method. The popularity of the method, as explained by Goringe et al. [48], stems from the view that the tight binding method combines physical



transparency and quantum mechanical sophistication, as well as being a method that combines computational speed with surprising accuracy. The same applies, in our view, to standard  $\pi$  Hückel MO theory, although in most practical molecular applications today the level of accuracy that's required cannot be achieved by such a simple model. It can, however, help us understand covalent bonding.

## 6. The quantum dynamical content of Hückel Theory

We have seen above that Hückel theory resolves covalent bonding in terms of a kinetic coupling allowing  $\pi$ -electrons to form delocalized molecular orbitals. Now we shall show how this in fact resolves the interatomic flow of electrons which can vary in extent (degree of delocalization) and rate. Thus the Hückel model can be seen as a simple theory of molecular electron dynamics. In turn we shall be able to deduce that covalent bonding is most generally understood as due to a quantum dynamical mechanism relating to the facilitation of interatomic electron transfer.

As suggested by the examples above, the Hückel  $\pi$ -MO-s of polyenes are expected to be delocalized. A simple, yet convincing way to demonstrate this is to utilize the analogy between Hückel theory and the finite element method (FEM) representation of wave functions of a "particle in a box", which is a familiar example to chemistry students. It is also known as the Free Electron Molecular Orbital (FEMO) model for conjugated  $\pi$  systems [42,50]. It represents the simplest quantum mechanical treatment of conjugated molecules, whereby the  $\pi$ -electrons are assumed to be fully delocalized within a one-dimensional box, the length of which is chosen on the basis of the total distance between the end-atoms of the conjugated system. The system, used also in our discussion of Thomas-Fermi theory above, is defined by the square-well potential:

$$V(x) = 0, \quad 0 < x < L \\ = \infty, \quad \text{elsewhere,} \quad (51)$$

and solution of the one-dimensional Schrödinger equation yields the following energy eigenvalues and (delocalized) eigenfunctions:

$$E_n = \frac{n^2 h^2}{8mL^2}, \quad (52)$$

$$\psi_n(x) = \sqrt{\frac{2}{L}} \sin \frac{n\pi x}{L}, \quad n = 1, 2, \dots, \infty, \quad (53)$$

where  $h$  is Planck's constant and  $m$  is the mass of the particle, i.e. here the electron.

An unusual but, in the context of this work, instructive way to solve this problem is to use the finite element method. This is a basis set method where, in the simplest implementation, the basis functions are *roof functions*, centred at equidistant grid-points  $\{x_k\}$ :

$$\phi_k(x) = \sqrt{\frac{3}{2\Delta}} \frac{(x - x_{k-1})}{\Delta}, \quad x_{k-1} < x < x_k, \quad (54)$$

$$\begin{aligned} &= \sqrt{\frac{3}{2\Delta}} \frac{(x_{k+1} - x)}{\Delta}, \quad x_k < x < x_{k+1} \\ &= 0, \quad \text{elsewhere.} \end{aligned}$$

The  $N$  basis functions (for  $N = 7$ ) are illustrated in Figure 19, and the grid-spacing  $\Delta$  is of course equal to  $L/(N + 1)$ .

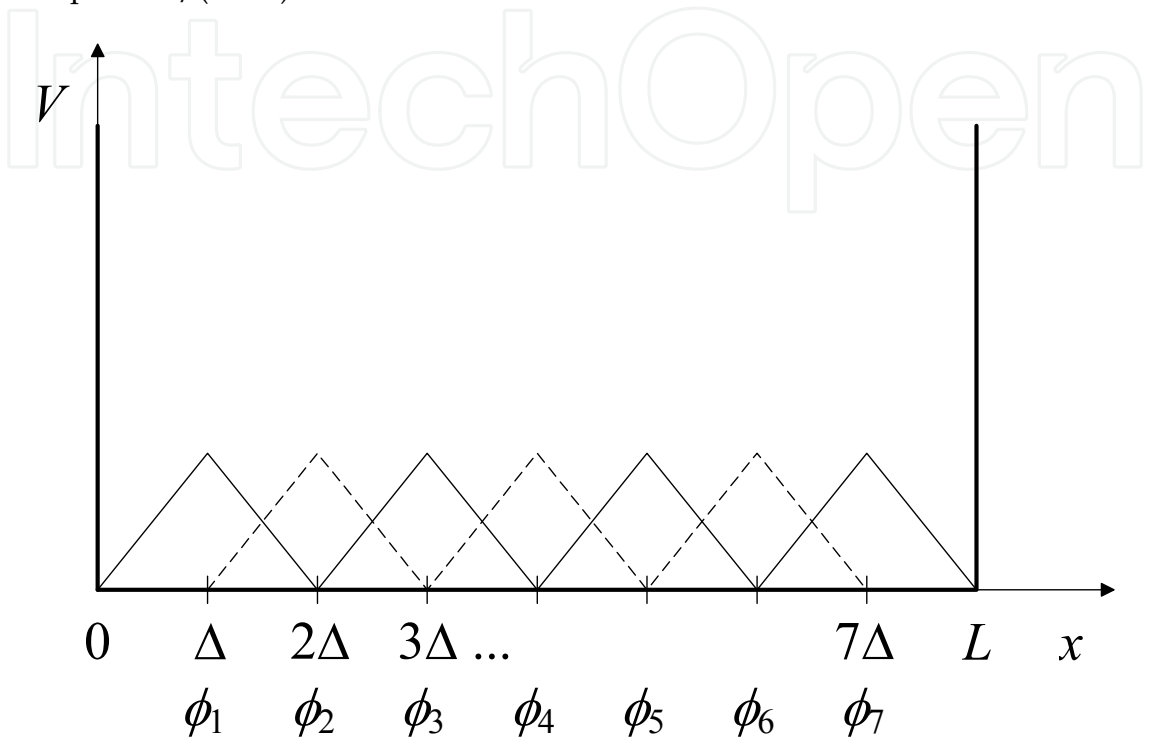


Fig. 19. Square well potential of particle in a box system showing grid-points and the FEM roof functions  $\{\phi_k\}$  for  $N = 7$ .

Note that these basis functions are normalized but not orthogonal. The overlap matrix  $\mathbf{S}$  is obtained by simple integration:

$$\begin{aligned} S_{kl} &= 1, \quad \text{if } k = l \\ &= 1/4, \quad \text{if } k = l \pm 1, \\ &= 0, \quad \text{otherwise.} \end{aligned} \tag{55}$$

The Hamiltonian consists of only the kinetic energy operator:

$$\hat{H} = -\frac{\hbar^2}{2m} \frac{d^2}{dx^2}, \tag{56}$$

and we obtain the Hamiltonian matrix elements via integration by parts (c.f. equation 36), whereby only the first derivatives of the roof functions are required. Thus,

$$H_{kl} = \frac{3}{2} \frac{\hbar^2}{m\Delta^2}, \quad \text{if } k = l, \tag{57}$$

$$\begin{aligned}
 &= -\frac{3}{4} \frac{\hbar^2}{m\Delta^2}, \quad \text{if } k = l \pm 1, \\
 &= 0, \quad \text{otherwise.}
 \end{aligned}$$

Now, we note that the structures of these translational Hamiltonian and overlap matrices in the FEM roof-function basis are precisely those of the *standard Hückel model with overlap* which we discussed above. Thus we merely identify the Hückel parameters as follows:

$$\alpha = \frac{3}{2} \frac{\hbar^2}{m\Delta^2}, \quad (58)$$

$$\begin{aligned}
 \beta &= -\frac{3}{4} \frac{\hbar^2}{m\Delta^2} = -\frac{\alpha}{2} \\
 \gamma &= \frac{1}{4}.
 \end{aligned}$$

The energy eigenvalues,  $\{\varepsilon_i\}$ , and the corresponding matrix of eigenvectors,  $\mathbf{C}$ , are given by equations (27) and (28). Since the basic form of the eigenvectors is independent of the magnitudes of the parameters  $\alpha$ ,  $\beta$  and  $\gamma$ , we can conclude that the Hückel eigenvectors for a linear polyene will be completely delocalized over the entire carbon back-bone of the molecule the same way as the eigenfunctions of the particle in a box.

It is worth noting that the eigenvalues,  $\lambda$ , and eigenvectors,  $\mathbf{U}$ , of the corresponding topology matrix,  $\mathbf{M}$ , can be written in analytic form [42]:

$$\lambda_n = -2 \cos \frac{n\pi}{N+1}, \quad (59)$$

$$U_{kn} = \sqrt{\frac{2}{N}} \sin \frac{nk\pi}{N+1} \quad (60)$$

$$= \sqrt{\frac{L}{N}} \psi_n(k\Delta),$$

where  $\psi_n$  is the  $n$ -th (exact) eigenstate of the particle in a box, as given by equation (53). The coefficients of the roof functions in a given global wave function  $\psi_n$  are thus the same as the coefficients for the  $2p_z$  AO-s at corresponding carbon sites in the Hückel scheme, all given by the numerical value of  $\psi_n$  evaluated at the grid-point in question. The analytic formulae in equations (59) and (60) actually found their way into the chemical literature as solutions of the Hückel equations for linear polyenes [42]. Analogous analytical formulae exist for (mono-) cyclic polyenes, where complete delocalization of the Hückel MO-s can be similarly demonstrated by analogy with the particle on a ring problem.

Since the eigenvectors of the particle in a box correspond to wave functions that are fully delocalized within the square well, the model describes free translation of the particle inside the box. In other words, if at some time  $t = 0$  the particle is represented by a localized wave-packet  $\xi(x, 0)$ , the time-evolution of the latter is given by

$$\xi(x, t) = \sum_n \langle \psi_n | \xi(x, 0) \rangle \exp(-iE_n t / \hbar) \psi_n(x) \quad (61)$$

and therefore the probability density,  $P(x, t)$ , of this wave packet evolves in time according to

$$P(x, t) = |\xi(x, t)|^2 = \sum_{n,l} \langle \psi_n | \xi(x, 0) \rangle \langle \xi(x, 0) | \psi_l \rangle \cos \frac{(E_n - E_l)t}{\hbar} \psi_n(x) \psi_l(x), \quad (62)$$

where the eigenfunctions,  $\{\psi_n\}$ , of the (time-independent) Hamiltonian, are assumed to be real.

As an illustration of the movement of a wave-packet, let it initially correspond to the first roof function,  $\phi_1$ , i.e.,

$$\xi(x, 0) = \phi_1(x). \quad (63)$$

The probability density at a given grid-point  $x_k$  at time  $t$  is then

$$P(x_k, t) = \sum_{n,l} (C_{1n} + \gamma C_{2n})(C_{1l} + \gamma C_{2l}) \cos \frac{(E_n - E_l)t}{\hbar} C_{kn} C_{kl}. \quad (64)$$

For  $N = 4$  the application of this equation (utilising equations (27), (28), (59) and (60) for the coefficients  $\{C_{kn}\}$  and energies  $\{E_n\}$ ) yields the results shown in Figure 20.

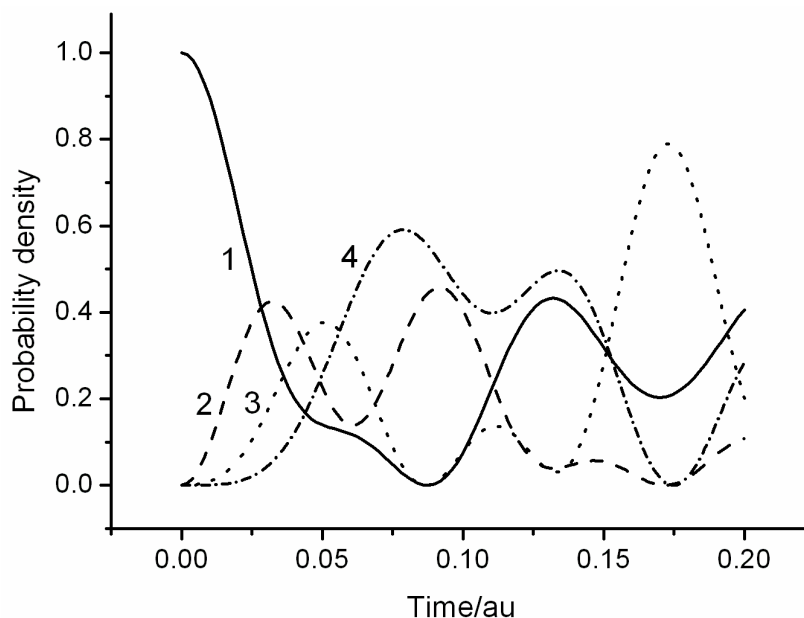


Fig. 20. Time evolution of probability density  $P(x_k, t)$  at a given grid-point  $x_k$  for a wave packet defined as the roof function  $\phi_1$  at  $t = 0$ , in a basis of 4 roof functions ( $N = 4$ ), with the grid-point index  $k$  shown in the figure.

The time-evolution of the densities at the four grid points within the box demonstrates the movement of density from one end of the box to the other including reflections from the

ends and the broadening of the initial wave packet. Since the time-independent eigenstates of the Hamiltonian are completely delocalized, an electron initially localized at one end of the box is able to freely traverse the box, i.e. fully access the available phase space. The time average of the probability density at a given grid-point is simply

$$\langle P(x_k) \rangle = \lim_{\tau \rightarrow \infty} \frac{1}{\tau} \int_0^{\tau} dt P(x_k, t). \quad (65)$$

Approximating the integral by discrete summation, we define  $\langle P(x_k) \rangle_{\tau}$  which represents the time average of the probability density calculated for a finite value of  $\tau$ . A plot of the computed values of  $\langle P(x_k) \rangle_{\tau}$  as a function of  $\tau$  for the current problem is shown in Figure 21. It provides a convincing illustration of the rapid convergence and uniformization of the probability densities at the various grid points. The fully converged values are  $\langle P(x_1) \rangle = \langle P(x_4) \rangle = 0.3$  and  $\langle P(x_2) \rangle = \langle P(x_3) \rangle = 0.2$ .

As shown above, the Hückel type Hamiltonian reflects translation which is free within the region spanned by the delocalized eigenfunctions. Hückel MO theory therefore describes the free translation of electrons among the atoms of the linear structures established by the carbon atoms of a planar conjugated hydrocarbon molecule, which form a “molecular wire”. The values of  $\beta$  and  $\gamma$  will give the moving electron an effective mass and a velocity. The shifts in orbital energies, downward for bonding MO-s, which brings about the energetic stabilization of the molecule, are clearly associated with the “delocalization of the electronic motion.” The fundamental mechanism of covalent bonding is therefore electron delocalization.

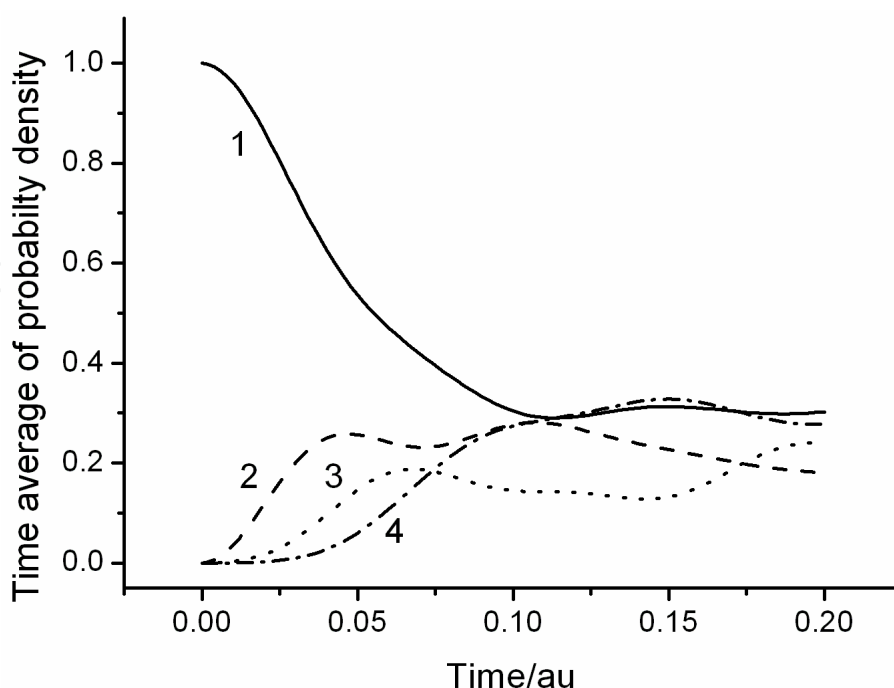


Fig. 21. Time averages of probability densities  $\langle P(x_k) \rangle_{\tau}$  as a function of the elapsed time  $\tau$ , with the grid-point index  $k$  shown in the figure.

## 7. Quantum Ergodicity and the Hückel Model

The Hückel model is about the coupling of carbon atoms, formation of delocalized molecular orbitals and electron translation along “molecular wires” but most of all it is about stabilization of  $\pi$ -bonded conjugated hydrocarbon molecules. Why does delocalization lead to stabilization? The answer can be given at different levels of explanation. The simplest answer may be to appeal to the Uncertainty Principle, as it clearly defines the connection between spatial localization and zero-point energy of a quantum particle. This relationship is particularly clearly demonstrated by the behaviour of a particle in a box, as summarized by equation (52), whereby the (kinetic) energy of the particle is inversely dependent on the size of the box,  $L$ . The more we localize particle motion, by reducing  $L$ , the higher the zero-point energy becomes along with increased spacing between energy levels, since

$$E_n - E_{n-1} = \frac{(2n+1)h^2}{8mL^2}. \quad (66)$$

Thus, it is clear that if the interaction of atoms results in delocalization of the valence electrons, then this must, in general, decrease the occupied orbital energies of the system and thereby its total energy, resulting in the formation of a molecule. This was discussed by Hellmann [9], who, although aware of the Virial Theorem, emphasised the drop in kinetic energy due to delocalization upon molecule formation. Reality is however a little more complex. As indicated in the Introduction, the accurate energetics of molecule formation (which satisfy the requirements of the Virial Theorem) appear to contradict Hellmann's ideas, because they also account for orbital contraction. As shown by Ruedenberg and co-workers [13, 38-41], the correct analysis of the energetics from the point of view of covalent bonding needs to separate the atomic orbital contraction effects from the molecular interference and delocalization effects.

At another, and possibly deeper level of explanation, we point out that the reactivity of atoms is related to the presence of nonergodic constraints which are relaxed as the molecule forms, thereby lowering the energy. The concept of quantum ergodicity is not widely known nor without subtlety. A classical (microcanonical) system is said to be ergodic if its trajectory dynamics uniformly accesses, or *covers*, all parts of the (momentum-position) phase space which are consistent with a given total energy. Following the original suggestion of von Neumann, it was proposed [51] that a quantum system is ergodic if and only if the spectrum of energy eigenstates is non-degenerate. Thus a system with a degenerate energy spectrum would be classified nonergodic. Subsequently it has been recognized that a *degree* of ergodicity could be discerned from the corresponding degree of regularity of the spectrum of energy eigenvalues, with an ergodic system displaying a smooth variation of energy gaps which translate into a corresponding smooth variation in the total density of states of the system [51]. By contrast, a nonergodic system would display random variations in the energy gaps. While there is no doubt about the validity of such a correlation between ergodic properties of a system and its spectral properties, we believe that quantum ergodicity is more directly related to the character of the energy eigenfunctions. This suggestion has been made and explored in earlier work on anharmonically coupled harmonic oscillators [52]. Consequently, the definition we adopt here is that a quantum system is ergodic if the energy eigenfunctions are maximally delocalized in any local basis set. The full implications of this

definition may not be immediately obvious. There are many conceivable local basis sets to examine and the meaning of “maximal delocalization” is not readily apparent either. However, in some cases the application of the above definition is straightforward. Such is the case with the Hückel model of conjugated polyenes, because the relevant local basis set is obviously the set of carbon  $2p_z$  AO-s which are used to construct the Hückel MO-s, as illustrated for benzene in Figure 22.

In the absence of the coupling the localized basis functions form degenerate sets of zeroth order energy eigenfunctions. The coupling transforms them into  $\pi$ -MO-s with a band of energies. The MO-s may be maximally delocalized or not, depending on the underlying molecular geometry. The larger the coupling and the greater the degree of delocalization, the broader the energy band becomes, with energy levels which are more evenly spaced. As the occupancy of the MO-s is in Aufbau manner, in order of increasing energy, the broader the band of energies, the greater the energetic stabilization. Thus, the ergodic character of the  $\pi$ -MO-s, being indicative of the degree of delocalization and rate of electron transfer, leads to maximal binding.

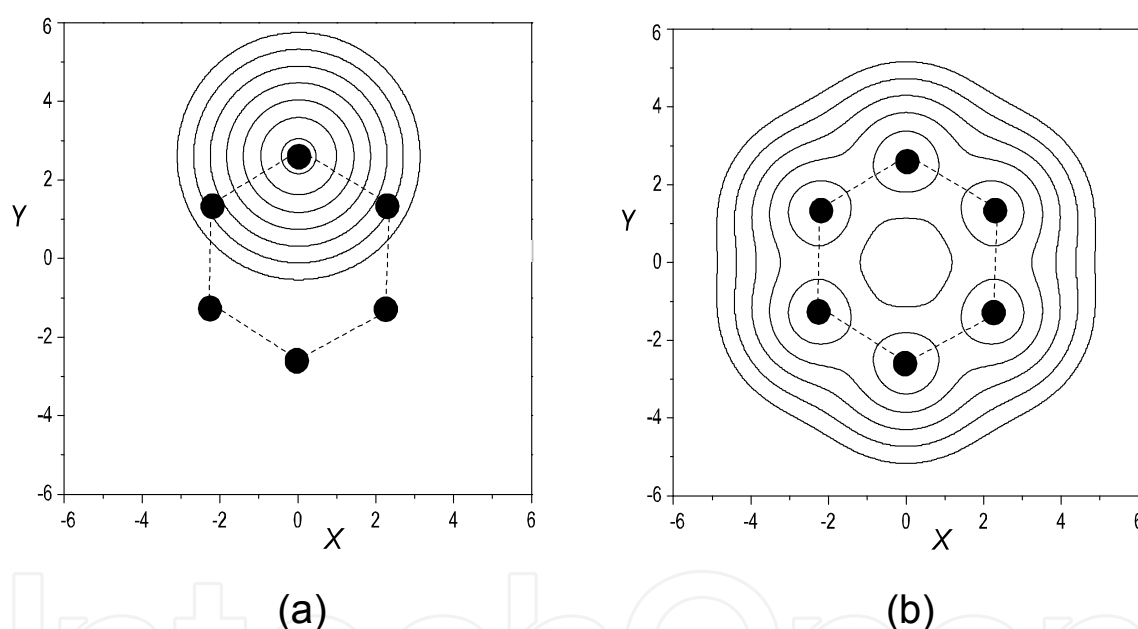


Fig. 22. Benzene: (a) Contour maps of  $2p_z$  AO, and (b) lowest energy Hückel  $\pi$ -MO displaying delocalization and maximal spread in terms of the localized basis. (Plane of contour map:  $0.32 a_0$  above molecular plane. Contour levels are  $0.002 \times 2^n$ ,  $n = 0, 1, 2, \dots$ )

A remarkable feature of the Hückel model is that the actual nature of the eigenstates is unaffected by the strength of the coupling. As indicated by equation (28), the relative contributions of the AO-s to a given MO is determined entirely by the topology of the molecule. The presence of overlap coupling between the AO-s only affects the normalization of the MO. Thus the slightest coupling leads to the formation of delocalized MO-s, as dictated by the topology of the molecule, which reflects a degree of ergodicity that is a geometrical feature, being independent of the coupling matrix element  $\beta$  and/or overlap  $\gamma$ . Only the rate of electron transfer among the atoms reflects the magnitude of the coupling. (Indeed, in the absence of any coupling, a polyene with  $n$  C-atoms would be  $n$ -fold



degenerate which would be unaffected by *any* unitary transformation of the AO basis, including the one that diagonalizes the topology matrix  $\mathbf{M}$  of the molecule.)

It should be clear then that from a fundamental quantum mechanical point of view covalent bond formation can be interpreted as the relaxation of dynamical constraints which make the non-bonded atoms or molecular fragments nonergodic. In  $\text{H}_2^+$  for example, the important constraint is the spatial confinement of the electron to the vicinity of one of the protons when the internuclear distance is large. As the distance decreases towards the equilibrium value the localization constraint is relaxed and the electron is able to more rapidly delocalize over the two protons. The same mechanism operates in the formation of the 2-electron  $\sigma$ -bond in  $\text{H}_2$  or the analogous  $\pi$ -bond in ethylene, but the process now involves two electrons of opposite spin. In the case of butadiene there is an additional stabilizing delocalization as the  $\pi$ -electrons are able to move along the whole chain of four carbon atoms. Similar additional delocalization is present in longer polyene chains and in cyclic molecules such as benzene. The covalent bonding mechanism in all these molecules is consistent with a more ergodic form of electron dynamics in the molecules than in the corresponding H atoms or in a hypothetical ethylene system without a  $\pi$ -bond ( $\beta = \gamma = 0$ ).

It is instructive to examine the character of the energy eigenstates of a polyene chain with reference to the ergodic hypothesis. The conventional valence-bond picture of a conjugated polyene is in terms of alternating single and double bonds between the carbon atoms, although the importance of delocalization is recognised by the introduction of *resonance* involving several canonical structures. In the Hückel MO model each carbon atom “donates” a  $2p_z$  AO towards the formation of delocalized  $\pi$ -MO-s, which are then occupied by the  $\pi$ -electrons of the molecule, one from each atom. Thus,  $\pi$ -bonding is delocalized right from the start, although it is customary to describe the individual CC bonds in terms of bond orders, which are readily obtained from the MO coefficients and which for a polyene typically range from  $\sim 0.5$  to  $\sim 0.8$ . As noted already, correction for non-zero overlap will renormalize the MO-s but will not affect the relative magnitudes of the coefficients. We claim that the Hückel eigenstates exhibit maximal delocalization in the  $2p_z$  AO basis. The support for this claim comes from the fact that the Hückel MO-s are formally equivalent to the particle-in-a-box eigenfunctions expanded in terms of roof functions, as discussed in the previous section. As this analogy has general applicability, we conclude that Hückel models of polyene chains exhibit full ergodicity and free translation of all electrons within the bounds established by the molecular chain.

In the case of cyclic polyenes, exemplified by benzene, the rotational symmetry and the cyclic boundary conditions impose restrictions which, as shown in Figure 17, result in two pairs of doubly degenerate (highest occupied and lowest unoccupied) MO-s. Such a pattern is typical of cyclic polyenes: Systems with an even number of carbon atoms have just two non-degenerate  $\pi$ -MO-s and only one, if the number of carbons is odd [42]. Application of the von Neumann definition to the latter would imply that the electron dynamics in cyclic polyenes is not fully ergodic. The degeneracies arise, however, as a result of the rotational character of electronic motion in systems with only cyclic boundary conditions and they correspond to the classical nonergodicity associated with the absence of reflection. Thus, the direction of motion, forward or backward, is an additional constant of motion. The motion is nonergodic for the trivial reason that direction cannot be reversed, but the rotation is still “free” in the sense that there are no barriers of any kind.

The analogous free electron MO model of cyclic systems is “the particle on a ring” whose energy eigenvalues and eigenfunctions are [42]

$$E_n = \frac{n^2 h^2}{8\pi I}, \quad (67)$$

$$\psi_n = \frac{1}{\sqrt{2\pi}} \exp(in\theta) \quad (68)$$

where  $n = 0, \pm 1, \pm 2, \dots$ ,  $I$  is the moment of inertia of the particle and  $\theta$  is the angular coordinate. With the exception of the ground state ( $n = 0$ ) all states are doubly degenerate, forming forward and backward rotating pairs of eigenstates at each energy.

## 8. Chemical bonding and delocalization

Recognizing the central role of delocalization in the quantum mechanical description of molecular electron structure, chemical bonding can be given a unified and physically correct description. We recognise that there are two separate sources of stabilization:

- i. Transfer of electrons due to differences in electronegativity, and
- ii. Delocalization of electronic motion.

In both cases the process of bonding brings the system towards ergodic and rapid electron dynamics. Due to the inherent asymmetry between bonded atoms in the former case, the ergodic dynamics in such systems is largely local, resulting in the type of interaction which, in the limiting case of complete charge transfer, we describe as ionic bonding. The covalent bonding mechanism, illustrated so clearly by the application of Hückel theory to polyenes, which implicitly accounts for resonance stabilization that is associated with conjugation and aromaticity, is a direct consequence of the relaxation of constraints which releases the bonding electrons to move freely among the bonded atoms of the molecule.

It is widely appreciated that ionic and covalent bonding represent two limiting bonding scenarios, with a continuous spectrum in-between, including bonds described as ionic bonds with covalent character, polar covalent bonds or covalent bonds with ionic character. Molecular orbital theory naturally covers all possible cases. This is most easily demonstrated by using perturbation theory to deduce the eigenvectors and eigenvalues (correct to first and second order respectively) of the following model Hamiltonian for a hypothetical heteronuclear diatomic molecule with two valence electrons, in a basis of two valence orbitals  $\phi_a, \phi_b$ , which are localized on the two atoms,  $a$  and  $b$ :

$$\mathbf{H} = \begin{pmatrix} \alpha & \beta \\ \beta & \alpha + \Delta\alpha \end{pmatrix}. \quad (69)$$

In this equation  $\Delta\alpha (>0)$  is nominally the difference in ionization energies of the two atoms, i.e. an energetic measure of their electronegativity difference. Assuming that  $\phi_a$  and  $\phi_b$  are orthogonal, the MO-s (in non-normalized form) and their energies are readily shown to be

$$\psi_a = \phi_a - \frac{\beta}{\Delta\alpha} \phi_b, \quad \psi_b = \phi_b + \frac{\beta}{\Delta\alpha} \phi_a, \quad (70)$$

$$\varepsilon_a = \alpha - \frac{\beta^2}{\Delta\alpha}, \quad \varepsilon_b = (\alpha + \Delta\alpha) + \frac{\beta^2}{\Delta\alpha}, \quad (71)$$

provided  $\beta/\Delta\alpha \ll 1$ . In the limiting case of very large electronegativity difference and sufficiently small coupling, i.e.  $\beta/\Delta\alpha \approx 0$ , the model predicts ionic bonding, whereby  $\psi_a$ , the lower energy MO, accommodating both electrons, is entirely localized on atom  $a$ . The energetic stabilization of the ion pair is of course due to the Coulomb attraction of the oppositely charged ions. For small but finite values of  $\beta/\Delta\alpha$ ,  $\psi_a$  contains some contribution from  $\phi_b$ , i.e. there is some delocalization, signalling a degree of covalent character to the predominantly ionic bond. These effects increase with decreasing  $\Delta\alpha$ , corresponding to increasing covalency (through the regime when low order perturbation theory is no longer applicable). In the limit of  $\Delta\alpha = 0$  we have a homonuclear diatomic with fully delocalized MO-s

$$\psi_{\pm} = \phi_a \pm \phi_b \quad (72)$$

and a fully covalent bond with the two electrons equally shared by the two atoms.

In extended systems, ranging from just triatomics such as  $\text{NO}_2$  to polyenes like benzene to crystalline solids such as graphite there is an increased degree of delocalization that can extend over the whole molecule, culminating in macroscopic delocalization that takes place in metallic systems such as solid sodium or graphite. Thus, metallic bonding is just a natural extension of the very basic covalent bonding mechanism that occurs in  $\text{H}_2^+$ ! The success and reliability of computational models based on MO theory to systems ranging from diatomics to proteins and to solids (in the form of the tight binding method briefly discussed above) provides convincing practical support for our belief that the MO model contains all the essential physics needed to correctly account for the wide range of bonding interactions of atoms and molecules that account for the chemistry of our world.

Depending on the system of interest and the accuracy we require of a specific calculation, the basic MO model may need to be extended so that the computed molecular wave function better approximates the exact wave function. This requires the use of large orbital basis sets as well the explicit inclusion of dynamical electron correlation, predominantly between electrons of opposite spins, which, by definition, is neglected in the Hartree-Fock formalism. For example, the quantitative prediction of a covalent bond dissociation energy requires the inclusion of correlation in the quantum chemical model since correlation contributions to bond dissociation energies are typically 25 - 50%. Another well-known deficiency of the (single configuration) Hartree-Fock method is its inability to correctly describe dissociation processes which involve the breaking of one or more two-electron covalent bonds, as occurs e.g. in the dissociation of  $\text{H}_2$  (from its ground state), which requires a multi-configuration treatment, i.e. the inclusion of non-dynamical (static) electron correlation. Irrespective, however, of the nature of the correlated wave function, whether it is multi-configuration SCF, configuration interaction or coupled cluster, it implicitly includes electron delocalization. This is obvious when a given correlated wave function is constructed in terms of delocalized MO-s, such as canonical SCF MO-s, or even localized SCF MO-s, e.g. two- or three-centre bond orbitals and lone pair orbitals, which, relative to the atomic orbitals, are of course considerably delocalized. Delocalization is less obvious when the total wave function is constructed directly from atomic orbitals, as in Valence

Bond Theory. For example, the Heitler-London wave function of  $H_2$  is built in terms of atomic configurations  $1s_a(1)1s_b(2)$  and  $1s_b(1)1s_a(2)$ . While these correspond to localized electrons (on atom  $a$  or  $b$ ), their (in-phase) combination, representing the ground state of  $H_2$ , is clearly a delocalized two-electron wave function.

## 9. Implications for Thomas-Fermi and modern Density Functional theories

We have seen above the direct relation between covalent bonding and valence electron dynamics which in turn is related to canonical orbital delocalization and energy splitting. The original Thomas-Fermi theory effectively assumes ergodicity of electronic motion and maximal transfer rates which in molecular orbital representation would mean maximally delocalized and energy separated canonical orbitals. Thus the atoms are according to the TF theory already relaxed into inert gas form and molecules are unstable since the effects on stability due to dynamical constraints posed by atomic shell structure and potential barrier hindrance of interatomic electron transfer cannot be resolved to favor molecule formation. Here we have emphasized the value of the understanding this failure provides concerning the mechanism of covalent bonding. The obvious follow up question is whether it is – given this understanding – possible to correct Thomas-Fermi theory and obtain a more useful but still “orbital free” form of TF-theory.

It is clearly possible to remove the assumed ergodicity with respect to spin-flipping as we have done here in our analysis of the hydrogen atom and the hydrogen molecular ion. It is also possible to recognize that quantization must be done separately and individually for the atoms of an infinitely expanded molecule. Thus we could immediately see that the energy of  $H_2^+$  would be lower at equilibrium separation than at infinite bond length where the energy should – with local quantization – be that of a hydrogen atom. In fact, we have in earlier work [4-7] explored the possibility of comparing traditional ergodic TF energies with nonergodic locally quantized TF energies to estimate the reactivity of atoms and the maximal stabilization possible by assuming that there were no dynamical constraints on the electronic motion for a molecule at its equilibrium geometry. This work was done using simplified exponential electron densities and empirical von Weiszäcker correction to allow atomic TF energies to agree with experiment or accurate quantum chemical results. The results have clearly shown that Thomas-Fermi theory, with or without spin and space localization imposed on the electronic motion and therefore also on the quantization, is capable of providing a measure of atomic reactivity and bonding efficiency in the formation of molecules. The picture one finds is in good agreement with chemical intuition. First row atoms are more reactive than those in the second row. Oxygen is the most reactive atom and – due to Pauli and internuclear repulsion and remaining constraints on electronic motion – only a small fraction (typically a quarter) of the stabilization energy available in principle is actually realized in the molecule at equilibrium.

An “orbital free” true density functional theory that can accurately predict reactivity and covalent bonding at all stages of molecule formation has still not been found. This is in itself a signal that covalent bonding is not – despite the Hohenberg-Kohn theorem [53] – readily described in terms of electron density. Wave functions, here in terms of one-electron orbitals, provide the best route to covalent bonding. The reason is, we hope, very clear from our analysis above: the canonical orbitals of Hartree-Fock, Hückel or modern density functional theory capture the character of the electron dynamics in the most direct manner and thereby



also reactivity and bonding. It has been noticed in connection with DFT applications to solids [54] that Thomas-Fermi theory can be corrected for the “nonbonding flaw” by a zeroth order orbital calculation where the one-electron Hamiltonian is generated from the Thomas-Fermi electron density and no iterations to consistency are performed. We have independently investigated such orbital corrections and verified [7] that the Thomas-Fermi results for electron densities of molecules can similarly be used to generate approximate one-electron Hamiltonians of the Fock or Kohn-Sham type which then yield energies of a quality nearly as good as that obtained by converging the corresponding Hartree-Fock or DFT calculations. This again illustrates the power of the molecular orbital analysis and the fact that it so effectively comprises and corrects the flaw of the Thomas-Fermi theory.

A final reflection on the evolution of modern DFT suggests that it is – perhaps surprisingly – more beholden to the Kohn-Sham method of estimating kinetic energy by an introduction of orbitals than it is to the Hohenberg-Kohn theorem which gave the density functional theory of electronic structure its legitimacy. Without a solution to the “nonbonding flaw” DFT would have remained of marginal interest in the great computational advance on molecular and solid state electronic structures over recent decades. The Kohn-Sham scheme inserted the molecular orbital analysis which – precisely as in the Hückel theory above or in the orbital correction of Thomas-Fermi theory – effectively resolved the electron dynamics and related mechanisms of reactivity and bonding. This suggests that improved functionals of either higher accuracy or computational efficiency must retain the ability to resolve the electron dynamics – if not by orbitals then by some other method no less able to describe the intimate coupling between electronic motion and stability.

## 10. Conclusions

The contrast between the total failure of the Thomas-Fermi theory and the success of the Hückel molecular orbital model in describing covalent bonding has shown very clearly that the mechanism of bonding is fundamentally of dynamical origin. Interatomic transfer of valence electrons, present to a degree in the molecule but absent between the separated atoms, relaxes the energy penalty of the constrained quantization in a dissociated molecule. The molecular orbitals obtained either by the application of Hückel theory, or by *ab initio* Hartree-Fock methods, capture the delocalization and orbital energy splitting which represent the spatial degree as well as the rate of valence electron transfer which underlies covalent stabilization. Thomas-Fermi theory employs an ergodic quantization scheme as if the delocalization and the rate of electron transfer were always maximal irrespective of bond lengths and potential and other barriers restraining such a flow. As soon as it is recognized that quantization must be done independently for separated atoms, Thomas-Fermi theory becomes capable of addressing reactivity and bonding. The non-bonding flaw is then identified, but without the use of molecular orbitals the quantitative prediction of covalent stabilization as a function of bond length is still too demanding for Thomas-Fermi theory. The obvious remedy to the problem was proposed by Kohn and Sham [55] in their famous prescription for the evaluation of kinetic energy. Our view is that the reintroduction of molecular orbitals, as in the Hückel model, provides the key to the quantitative representation of the valence electron dynamics and its effect on covalent stability.

The dynamical mechanism of covalent bonding as described above allows us to understand why earlier explanations of covalent bonding as due either to kinetic energy lowering or

electrostatic potential stabilization through electron density redistribution and build up of density around bond midpoints have led to persistent disputes. Both these mechanisms play a vital but subsidiary role to the dynamical relaxation which is the fundamental mechanism of covalent stabilization. Thus there are molecules with particular electronic structures and/or wave functions obtained by specific quantum chemical methods for which the description of bonding may agree or disagree with either of these earlier explanations of covalent bonding. This is because the fundamental valence electron transfer between atomic centres in the molecule may result in either potential or kinetic energy lowering which in themselves represent stabilization processes, but which are nevertheless less general than the underlying dynamical mechanism. Only the most general description of the mechanism will give us the full benefit of understanding the bonding seen in all types of molecules and computational methods.

Our analysis above has focused on the qualitative understanding of covalent bonding but we are convinced that a gain in such understanding will also bring advantages in the quantitative prediction of bonding. There are good reasons to believe that such benefits will first be found in the development of new density functional methods with improved performance with respect to computational efficiency and accuracy. Our work so far indeed contains a number of suggestions for the improvement of DFT and we look forward to much further progress in the future.

## 11. Acknowledgements

We thank our former graduate students and colleagues William Eek and Andreas Bäck for their many contributions to our earlier work some of which has specifically been drawn upon in the analysis above. The support of the Swedish Science Research Council over a long period, while this work was carried out, is also gratefully acknowledged.

## 12. References

- [1] Nordholm, S. J. *Chem. Phys.* 1987, 86, 363.
- [2] Nordholm, S. J. *Chem. Ed.* 1988, 65, 581.
- [3] Bacskay, G. B.; Reimers, J. R.; Nordholm, S. J. *Chem. Ed.* 1997, 74, 1494.
- [4] Eek, W.; Nordholm, S. *Theor. Chem. Acc.* 2006, 115, 266.
- [5] Nordholm, S.; Bäck, A.; Bacskay, G. B. *J. Chem. Ed.* 2007, 84, 1201 and Supplementary Information.
- [6] Nordholm, S.; Eek, W. *Int. J. Quant. Chem.* 2011, 111, 2072.
- [7] Eek, W. *Understanding Atoms and Covalent Bonds*, PhD thesis, The University of Gothenburg, 2008.
- [8] Lewis, G. N. *J. Am. Chem. Soc.* 1916, 38, 762.
- [9] Hellmann, H. *Z. Phys.* 1933, 85, 180.
- [10] Coulson, C. A. *Valence*, 2nd ed.; Oxford University Press: London, 1961.
- [11] Burdett, J. K. *Chemical Bonds - A Dialog*; Wiley: Chichester, 1997; Chapter 1.
- [12] Bader, R. F. W.; Hernandez-Trujillo, J.; Cortés-Guzman, F. J. *Comput. Chem.* 2007, 28, 4.
- [13] Ruedenberg, K. *Rev. Mod. Phys.* 1962, 34, 326.

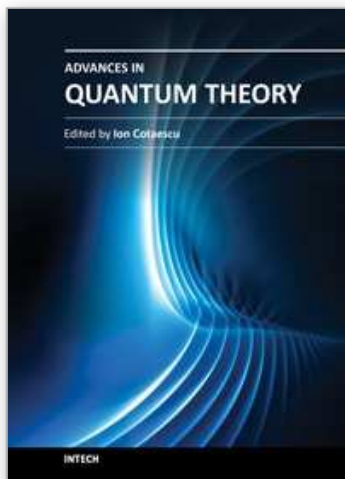
- [14] Kutzelnigg, W. In *Theoretical Models of Chemical Bonding*; Maksič, Z. B., Ed.; Springer: Berlin, 1990; p.1.
- [15] Bitter, T; Ruedenberg, K.; Schwarz, W. H. E. J. *Comput. Chem.* 2007, 28, 411.
- [16] Kutzelnigg, W. *Angew. Chem. Internat. Ed.* 2007, 28, 25.
- [17] Esterhuysen, C.; Frenking, G. *Theor. Chem. Acc.* 2004, 111, 381.
- [18] Thomas, L. H. *Proc. Cambridge Philos. Soc.* 1926, 23, 542.
- [19] Fermi, E. *Rend. Accad. Lincei* 1927, 6, 602.
- [20] Hückel, E. *Z. Phys.* 1930, 60, 423; *ibid.* 1931, 70, 204; *ibid.* 1931, 72, 310; *ibid.* 1932, 76, 628.
- [21] Teller, E. *Rev. Mod. Phys.* 1962, 34, 627.
- [22] Balazs, N. L. *Phys. Rev.* 1967, 156, 42.
- [23] Kutzelnigg, W. *J. Comput. Chem.* 2007, 28, 25.
- [24] Parr, R. G.; Yang, W. *Density Functional Theory of Atoms and Molecules*, Oxford University Press, New York, 1994.
- [25] von Weizsäcker, C. F. *Z. Phys.* 1935, 96, 431.
- [26] Ruedenberg, K. *J. Chem. Phys.* 1961, 34, 1861.
- [27] Longuet-Higgins, H. C.; Salem, L. *Proc. Roy. Soc. (London) A*, 1959, 251, 172.
- [28] Pople, J. A.; Walmsley, S. H. *Mol. Phys.* 1962, 5, 15.
- [29] Su, W. P.; Schriber, J. R.; Heeger, A. J. *Phys. Rev. Lett.* 1979, 42, 1698.
- [30] Klimkäng, A.; Larsson, S. *Chem. Phys.* 1994, 189, 25.
- [31] Larsson, S.; Rodriguez-Monge, L. *Int. J. Quant. Chem.* 1998, 67, 107.
- [32] Blomgren, F.; Larsson, S. *Theor. Chem. Acc.* 2003, 110, 165.
- [33] Coulson, C. A.; O'Leary, B.; Mallion, R. B. *Hückel Theory for Organic Chemists*; Academic Press: London, 1978.
- [34] Wheland, G. W. *J. Am. Chem. Soc.* 1942, 64, 900.
- [35] Parr, R. G. *J. Chem. Phys.* 1960, 33, 1184.
- [36] Löwdin, P.-O. *J. Chem. Phys.* 1950, 18, 365.
- [37] Weber, W.; Thiel, W. *Theor. Chem. Acc.* 2000, 103, 495.
- [38] Feinberg, M. J.; Ruedenberg, K.; Mehler, E. L. In *Advances in Quantum Chemistry*, Vol. 5; Löwdin, P. O., Ed.; Academic Press: New York, 1970; p. 28.
- [39] Feinberg, M. J.; Ruedenberg, K. *J. Chem. Phys.* 1971, 54, 1495.
- [40] Feinberg, M. J.; Ruedenberg, K. *J. Chem. Phys.* 1971, 55, 5804.
- [41] Ruedenberg, K. in *Localization and Delocalization in Quantum Chemistry*; Chalvet, O.; Daudel, R.; Diner, S.; Malrieu, J. P. Eds.; Reidel: Dordrecht, 1975; p. 223.
- [42] Pilar, F. L. *Elementary Quantum Chemistry*; McGraw-Hill: New York, 1968.
- [43] Pariser, R.; Parr, R. G. *J. Chem. Phys.* 1953, 21, 466; *ibid.* 1953, 21, 767.
- [44] Pople, J. A.; *Trans. Farad. Soc.* 1953, 49, 1375;
- [45] Pople, J. A. *J. Phys. Chem.* 1957, 61, 6.
- [46] Hoffmann, R. *J. Chem. Phys.* 1963, 39, 1397.
- [47] Wolfsberg, M.; Helmholz, L. *J. Chem. Phys.* 1959, 20, 837.
- [48] Goringe, C. M.; Bowler, D. R.; Hernández, E. *Rep. Prog. Phys.* 1997, 60, 1447.
- [49] Slater, J. C.; Koster, G. F. *Phys. Rev.* 1954, 94, 1498.
- [50] Baylis, N. S. *Quart. Rev.* 1952, 6, 319.
- [51] Jancel, R. *Foundations of Classical and Quantum Statistical Mechanics*; Pergamon Press: London, 1969.



- [52] Nordholm, S.; Rice, S. A. *J. Chem. Phys.* 1974, 61, 203.
- [53] Hohenberg, P.; Kohn, W. *Phys. Rev.* 1964, 136, B864.
- [54] Zhou, B.; Wang, Y. A. *J. Chem. Phys.* 2006, 124, 081107.
- [55] Kohn, W.; Sham, L. J. *Phys. Rev.* 1965, 140, A1133.

IntechOpen

IntechOpen



### **Advances in Quantum Theory**

Edited by Prof. Ion Cotaescu

ISBN 978-953-51-0087-4

Hard cover, 248 pages

**Publisher** InTech

**Published online** 15, February, 2012

**Published in print edition** February, 2012

The quantum theory is the first theoretical approach that helps one to successfully understand the atomic and sub-atomic worlds which are too far from the cognition based on the common intuition or the experience of the daily-life. This is a very coherent theory in which a good system of hypotheses and appropriate mathematical methods allow one to describe exactly the dynamics of the quantum systems whose measurements are systematically affected by objective uncertainties. Thanks to the quantum theory we are able now to use and control new quantum devices and technologies in quantum optics and lasers, quantum electronics and quantum computing or in the modern field of nano-technologies.

#### **How to reference**

In order to correctly reference this scholarly work, feel free to copy and paste the following:

Sture Nordholm and George B. Bacskay (2012). The Role of Quantum Dynamics in Covalent Bonding – A Comparison of the Thomas-Fermi and Hückel Models, *Advances in Quantum Theory*, Prof. Ion Cotaescu (Ed.), ISBN: 978-953-51-0087-4, InTech, Available from: <http://www.intechopen.com/books/advances-in-quantum-theory/the-mechanism-of-covalent-bonding-the-role-of-interatomic-electron-transfer-as-seen-in-a-comparison->

**INTECH**  
open science | open minds

#### **InTech Europe**

University Campus STeP Ri  
Slavka Krautzeka 83/A  
51000 Rijeka, Croatia  
Phone: +385 (51) 770 447  
Fax: +385 (51) 686 166  
[www.intechopen.com](http://www.intechopen.com)

#### **InTech China**

Unit 405, Office Block, Hotel Equatorial Shanghai  
No.65, Yan An Road (West), Shanghai, 200040, China  
中国上海市延安西路65号上海国际贵都大饭店办公楼405单元  
Phone: +86-21-62489820  
Fax: +86-21-62489821

© 2012 The Author(s). Licensee IntechOpen. This is an open access article distributed under the terms of the [Creative Commons Attribution 3.0 License](https://creativecommons.org/licenses/by/3.0/), which permits unrestricted use, distribution, and reproduction in any medium, provided the original work is properly cited.

IntechOpen

IntechOpen